Fruit Research

ARTICLE

Open Access

https://doi.org/10.48130/frures-0025-0025

Fruit Research **2025**, 5: e033

Molecular evolutionary analysis and expression patterns of nitrogen assimilation-related gene families in *Lycium ruthenicum* under salt stress

Jianwei Qi[#], Jun Zhao[#], Songsong Lu[*], Qianwen Song, Luna Xing, Weibo Du, Xiaowei Zhang, Xiaolei Zhou and Yanjun Ma[*]

Forest College of Gansu Agricultural University, Lanzhou 730070, Gansu, China

[#] Authors contributed equally: Jianwei Qi, Jun Zhao

[*] Corresponding authors, E-mail: luss86_gsau@163.com; mayanjun@gsau.edu.cn

Abstract

Nitrogen assimilation plays a critical role in the response of plants to salt stress. In this study, bioinformatics and computational biology methods were employed to identify members of the *Lycium GS*, *GOGAT*, and *GDH* gene families, and analyzed their expression patterns and transcriptional regulatory networks under salt stress in black wolfberry (*Lycium ruthenicum*). In addition, the adaptive evolutionary mechanisms of the black wolfberry *Fd-GOGAT* gene were explored. The results showed that the genomes or transcriptomes of *Lycium* species contain two to four *GS* genes, two *GOGAT* genes, and three to four *GDH* genes. Following NaCl stress, the expression of *Fd-GOGAT* and *NADH-GOGAT* in the leaves of black wolfberry was downregulated with increasing time and NaCl concentration; in the roots, *Fd-GOGAT* and *NADH-GOGAT* were upregulated by 1.79-fold and 1.40-fold, respectively, 12 h after severe NaCl stress. *GS2* and *GS1.1* are highly expressed in leaves and roots, respectively, and their expression is significantly upregulated under NaCl stress. The expression of *GDH* in leaves is downregulated under salt stress, whereas in roots, the expression of *NADP-GDH* and *GDH2* is upregulated under NaCl stress. *C2H2-63*, a key transcription factor regulating nitrogen assimilation in black wolfberry under salt stress, is likely to promote nitrogen assimilation through its upregulated expression. Additionally, seven positively selected sites (p.Glu220, p.Ala388, p.Ala880, p.Ser921, p.Leu1319, p.Ser1350, and p.Ser1570) were found in the *Fd-GOGAT* protein of black wolfberry. Compared to Ningxia wolfberry (*L. barbarum*), these mutation sites enhance the affinity of *Fd-GOGAT* for its substrate Glu, which helps to increase the catalytic efficiency of *Fd-GOGAT* in black wolfberry under salt stress. In conclusion, the adaptation of salt stress-related nitrogen assimilation genes in black wolfberry involves both gene expression regulation and adaptive evolution. Enhancing the GS/GOGAT pathway under salt stress is a primary strategic choice for nitrogen assimilation in black wolfberry.

Citation: Qi J, Zhao J, Lu S, Song Q, Xing L, et al. 2025. Molecular evolutionary analysis and expression patterns of nitrogen assimilation-related gene families in *Lycium ruthenicum* under salt stress. *Fruit Research* 5: e033 https://doi.org/10.48130/frures-0025-0025

Introduction

Salt stress negatively impacts plant growth and development, primarily disrupting their productivity and survival in arid and semi-arid regions worldwide[1]. It affects various physiological processes in plants, including seed germination, biomass production, reproductive growth, photosynthesis, nitrogen metabolism, stomatal regulation, and carbohydrate metabolism[2]. Nitrogen plays a crucial role in plant metabolism, as all key processes depend on proteins, of which nitrogen is a vital component[3]. Nitrogen deficiency affects plant growth, carbon fixation, leaf gas exchange, chlorophyll fluorescence parameters, thylakoid membrane structure, carbohydrate levels, metabolites, and seedling respiratory enzymes, among other processes[4,5]. Adequate nitrogen absorption and assimilation are beneficial for plant growth and resistance to salt stress. Nitrate and ammonium are the two main inorganic nitrogen sources for plants. Nitrate, once absorbed by the roots, is reduced to ammonium by nitrate reductase (NR) and nitrite reductase (NiR), and subsequently enters the glutamine synthetase (GS, EC 6.3.1.2)/glutamate (Glu) synthase (GOGAT, EC 1.4.7.1) cycle for assimilation into organic nitrogen. In contrast, ammonium directly enters the GS/GOGAT cycle to participate in the formation of organic nitrogen[6,7]. Specifically, GS catalyzes the production of glutamine from ammonium and Glu, while GOGAT catalyzes the conversion of glutamine and 2-oxoglutarate (2-OG) to produce two molecules of Glu. One molecule of Glu can serve as a substrate for GS, and the other can be used for the synthesis of proteins, nucleic acids, and other nitrogen-containing compounds[8]. Numerous studies have demonstrated that salt stress affects nitrification and ammonification processes in soil, as chloride (Cl^-) competes with nitrate (NO_3^-) and leads to ion toxicity and ion imbalance, which explicitly restricts nitrogen uptake, transport, and assimilation processes[9]. Therefore, the GS/GOGAT cycle is essential for maintaining nitrogen use efficiency (NUE) in plants under salt stress[10]. It is well known that varieties capable of maintaining high GS/GOGAT activity exhibit greater resistance to salt stress[11]. However, under salt stress conditions, the enzymatic activities of GS and GOGAT are reduced in most plants, which limits amino acid production and can lead to increased accumulation of NH_4^+. The accumulation of NH_4^+ in a saline environment has been reported to trigger the activation of the alternative glutamine dehydrogenase (GDH, EC 1.4.1.2) pathway for its assimilation[12]. In various studies, the accumulation of NH_4^+ has been observed to coincide with a sharp increase in GDH activity. This alternative pathway can be considered a mechanism of salt tolerance[13].

GOGAT is a key rate-limiting enzyme in the GS/GOGAT cycle. In plants, Glu synthase primarily exists in two forms: Fd-GOGAT, which uses ferredoxin (Fd) as an electron donor, and NADH-GOGAT, which uses NADH as an electron donor[14]. In most crops, salt stress inhibits GOGAT activity and gene expression. For instance, in cucumber and *Populus simonii*, salt stress significantly suppresses GOGAT activity, leading to a marked reduction in nitrogen assimilation rates[15,16]. However, compared to salt-sensitive varieties, salt-tolerant varieties

maintain higher GOGAT activity and transcript levels under salt stress[17–19]. This suggests that maintaining high GOGAT expression is crucial for enhancing nitrogen assimilation rates under salt stress. In higher plants, GS exists as two distinct isoforms: cytosolic GS1 and plastidic GS2. GS1 is encoded by a multigene family, while GS2 is encoded by a single nuclear gene. Transgenic rice plants overexpressing GS2 (plastidic) exhibit enhanced photorespiration and salt tolerance under salt stress conditions[20]. Therefore, GS positively regulates plant tolerance to salt stress by enhancing the rate of nitrogen assimilation. The GDH gene family in plant genomes typically contains three to four members, including both NAD- and NADP-dependent forms. The reactions catalyzed by GDH are reversible. Studies on *Casuarina glauca* have revealed that GDH2 in *Frankia* plant shoots is significantly upregulated under salt stress across three salt treatment gradients, indicating that plants respond to salt stress by activating the GDH pathway[21]. Numerous transcription factors regulate the NUE of plants. The overexpression of the DNA-binding single finger protein 1 (Dof1) transcription factor appears to enhance nitrogen uptake and assimilation in plants under low nitrogen conditions. Dof1 is a key activator of several genes involved in organic acid metabolism. Studies overexpressing maize Dof1 in *Arabidopsis* have shown that plant growth improves under low nitrogen conditions, with increased levels of amino acids (glutamine and Glu) and total nitrogen content[22]. Recent experiments overexpressing ZmDof1 in rice have demonstrated that under nitrogen-limited conditions, transgenic rice plants exhibit increased nitrogen and carbon accumulation, as well as enhanced photosynthesis rates. Nitrogen accumulation is particularly pronounced in the roots, and the biomass of these roots is higher than that of control plants. Additionally, experiments have found that C2H2, AP2, and NAC transcription factors are also involved in the nitrogen assimilation processes in plants. TaZFP1, a C2H2 type-ZFP gene of *T. aestivum*, mediates salt stress tolerance of plants by modulating diverse stress-defensive physiological processes[22].

Black wolfberry (*Lycium ruthenicum*) is a perennial halophytic shrub belonging to the Lycium genus in the Solanaceae family. It possesses characteristics such as salt and drought tolerance and is an endemic species in the saline-alkali desert regions of northwestern China[23]. Multi-omics research has revealed that under salt stress, the differentially expressed genes and metabolites in black wolfberry leaves are significantly enriched in nitrogen metabolism pathways, suggesting that nitrogen metabolism plays an important role in the plant's response to salt stress[24]. Additionally, under high concentrations of NaCl stress, the proline content in the roots and stems of both black wolfberry and Ningxia wolfberry (*L. barbarum*) increases significantly, with black wolfberry consistently exhibiting higher proline levels than Ningxia wolfberry[25]. Research has shown that under salt stress, the biosynthesis of proline primarily occurs through a pathway that uses Glu as a substrate[26]. These findings suggest that black wolfberry may resist salt stress by enhancing its nitrogen assimilation processes. However, to date, the genetic basis of the key nitrogen assimilation genes *GOGAT*, *GS*, and *GDH* in black wolfberry, as well as whether black wolfberry maintains a high nitrogen assimilation rate under salt stress, remains unclear. Therefore, this study employs bioinformatics and computational biology methods, utilizing the transcriptome data of black wolfberry under different NaCl stress concentrations from our research group, to analyze the transcriptional regulatory patterns of *GOGAT*, *GS*, and *GDH* genes in black wolfberry under NaCl stress. Furthermore, based on the results of molecular evolutionary analysis, the impact of Fd-GOGAT mutation sites on protein function is discussed, providing a reference for further studies on the role of nitrogen assimilation-related genes in the salt tolerance of black wolfberry.

Materials and methods

Data sources

The whole genome sequences and annotation files of Ningxia wolfberry (*L. barbarum*), African boxthorn (*L. ferocissimum*), and tomato (*Solanum lycopersicum*) were downloaded from the NCBI database (www.ncbi.nlm.nih.gov) on March 5, 2024. The respective version numbers for these genomes are ASM1917538V2, AGI_CSIRO_Lferr_CH_V1, and SL4.0. The black wolfberry genome, designated as 'Final', was obtained from the Figshare repository (https://figshare.com). Additionally, transcriptome data for Chinese wolfberry (*L. chinense*) and white-fruited *L. ruthenicum* were obtained from NCBI for transcript assembly, with the accession numbers SRR12805582 and SRR18059520, respectively. The transcript assembly for *L. chinense*, the white fruit of *L. ruthenicum,* was performed using Trinity (version 2.15.1)[27] with default parameters.

Bioinformatics analysis of the *GOGAT* gene family in *Lycium* species

Identification of GOGAT gene family members

The CDS sequences of tomato *GOGAT* genes were downloaded from the SOL Database (http://solgenomics.net/, accessed on 5 March 2024). The downloaded tomato *GOGAT* genes were then aligned to the tomato genome using BLAST (2.16.0) to verify the accuracy of the annotation information. The accurately identified tomato *GOGAT* genes were subsequently aligned to the genomes or transcriptomes of *Lycium* species to obtain candidate *GOGAT* genes in *Lycium* species. Finally, the resulting candidate genes were aligned to the Non-Redundant Database/Nucleotide Sequence Database (NR/NT) to confirm the accuracy of the identification results. The identification method for *GS* and *GDH* was consistent. The protein sequences of the *GS* and *GDH* genes were downloaded from the Arabidopsis official database (TARE: www.arabidopsis.org). The *AtGS* and *AtGDH* PFAM models were constructed using hmmbuild. Subsequently, the *AtGS* and *AtGDH* PFAM models were used to search for protein sequences containing the characteristic domains of *GS* and *GDH* in the tomato genome, with a sequence screening threshold of E-value < 0.001. Then, the tomato *GS* and *GDH* sequences were used to build PFAM models, which were subsequently employed to search the genomes of *Lycium* species in order to identify the *GS* and *GDH* genes in *Lycium* species. Finally, the presence of characteristic domains was further verified in the NCBI-CDD database (www.ncbi.nlm.nih.gov/structure/bwrpsb/bwrpsb.cgi).

Phylogenetic relationships, gene structure, and motif analysis

Based on the identification results of *GOGAT, GS,* and *GDH* gene family members in *Lycium* species and tomato, the CDS sequences of each gene were selected for phylogenetic tree construction. The phylogenetic relationships of the *GOGAT, GS,* and *GDH* genes from the six species mentioned above were inferred using IQ-Tree (2.3.4)[28] based on the maximum likelihood method, with the nucleotide substitution model set to TIM2+F+G4, Blosum62+F+G4, and Blosum62+F+G4. Gene structures were visualized using GSDS (https://gsds.gao-lab.org, accessed on 12 April 2024)[29]. Motif prediction was performed using MEME (https://meme-suite.org/meme/info/status?service=MEME&id=appMEME_5.3.31625885416694-401203024, accessed on 27 April 2024), with a significance threshold of $p < 0.05$.

Analysis of the physicochemical properties of proteins

The physicochemical properties of the polypeptide chains corresponding to the proteins of *Lycium* species were predicted using the online software Expasy (https://web.expasy.org/protparam/,

accessed on 12 May 2024). The predicted properties include the number of amino acids, molecular weight (Da), isoelectric point (pI), GRAVY index, and instability index.

Transcriptional regulatory analysis

The upstream 2,000 bp regulatory region sequence of the black wolfberry *GS, GOGAT,* and *GDH* genes was extracted, and the PlantTFDB database (https://planttfdb.gao-lab.org/, accessed on 1 June 2025)[30] was utilized to predict the binding sites of transcription factors. The transcriptional regulatory network was constructed using Cytoscape (version 3.10.0)[31]. Protein-protein interactions were predicted using STRING software (https://cn.string-db.org/cgi/input?sessionId=bybyzz3LRoB1&input_page_show_search=on) with tomato set as the reference species at a confidence threshold of 0.9. The network visualization was subsequently refined using Cytoscape software.

Transcription factor-DNA docking analysis

The DNA-binding domains of transcription factors were predicted using PlantTFDB. The binding sites of transcription factors on the DNA sequence were predicted using JASPAR (https://jaspar.elixir.no/inference, accessed on 3 June 2025). The docking conformation of the transcription factor-DNA complex was predicted using the Alphafold3 server (https://alphafoldserver.com/, accessed on 3 June 2025)[32]. The interactions at the transcription factor-DNA interface were analyzed using PDBePISA (www.ebi.ac.uk/pdbe/pisa/, accessed on 4 June 2025). Visualization was performed using PyMOL 3.1[33].

Transcriptomic analysis of black wolfberry root and leaf tissues under salt stress

Material processing and transcriptomic analysis

The plant materials used were black wolfberry tissue culture seedlings preserved in the Tissue Culture Laboratory of the Forestry College at Gansu Agricultural University. The cultivation conditions were as described by Wei et al.[34]. Healthy and vigorous seedlings were selected and cultured in 1/2 Hoagland's solution. When the seedlings reached 14 d of growth, NaCl solutions were added at concentrations of 0, 50, and 250 mmol/L. The roots and leaves of the seedlings from each NaCl concentration were sampled at 0, 1, and 12 h post-treatment for transcriptomic sequencing. Each treatment was replicated in triplicate. Clean reads were aligned to the black wolfberry transcriptome using Hisat2 (2.2.1)[35]. Gene alignment quantification was performed using featureCounts (2.0.3)[36], and the Fragments Per Kilobase of transcript per Million mapped reads (FPKM) value for each gene was calculated based on gene length. Differential expression analysis between the two groups was conducted using DESeq2 (1.22.1)[37], with the Benjamini & Hochberg method employed to adjust the *p*-values. Genes with adjusted *p*-values (FDR) and |log2FoldChange(FC)| > 1 were considered to be significantly differentially expressed.

Expression level of the GS, GOGAT, and GDH gene in black wolfberry under salt stress

Extract the expression data of the *GS, GOGAT,* and *GDH* genes and related transcription factors in black wolfberry under salt stress. Use one-way ANOVA in SPSS 22.0 to assess the significance of differences ($p < 0.05$) among different treatments and treatment times. Visualization was performed using Origin 2021. The K-means analysis of transcriptional factor expression patterns was performed using the stats package in R version 4.2.0. The data were normalized using the log2 transformation, while all other parameters were set to their default values[38].

Identification of transcription factors in black wolfberry

Transcription factors in black wolfberry transcripts were identified using the PlantTFDB database (https://planttfdb.gao-lab.org/).

Molecular evolutionary analysis and comparative protein structure analysis

Molecular evolutionary analysis

The molecular evolutionary analysis was conducted as described by Qi et al.[39]. Specifically, the branch-site model from PAML 4 (v4.9j)[40] was employed to analyze the selective pressure and identify positive selection sites within each member of the black wolfberry *GS*, *GOGAT,* and *GDH* gene family. The Bayesian Empirical Bayes (BEB) method was used to calculate the probability of positive selection sites. Additionally, likelihood ratio tests (LRTs) were performed to assess the significance of the difference between Model A0 and Model A1, and a significance threshold of 0.05 was applied.

Protein model construction and quality assessment

A homology template search for the black wolfberry Fd-GOGAT protein was conducted using the SWISS-model module (https://swissmodel.expasy.org/interactive, accessed on 17 August 2024). Based on the search results, the crystal structure of the *Synechocystis* sp. GOGAT protein (1LLW, 2.70Å) was selected as the template for homology modeling. Subsequently, the Modeller[41] software was utilized for single-template modeling to predict the monomeric structure of the Fd-GOGAT protein. The parameters were set to predict 100 models, and the optimal model was selected using the DOPE and GA341 scoring functions. The quality of the constructed model was assessed using the online software SAVES v6.0 (https://saves.mbi.ucla.edu/, accessed on 17 August 2024). A model was considered acceptable if more than 90% of the amino acid residues fell within the 'red zone'. Homology structure comparison and 3D structure visualization were performed using UCSF Chimera (1.16)[42], and VMD (1.9.4) software.

Protein structure comparison

The hydrophilicity of the polypeptide chain amino acid residues was predicted using ProtScale (https://web.expasy.org/protscale/), with the method set to Hphob./Kyte & Doolittle. Potential positively selected sites were subjected to single-point mutation prediction using the online tool Missense 3D[43] (http://missense3d.bc.ic.ac.uk/missense3d/). Molecular docking of Fd with the substrate glutamine was performed using AutoDock (4.2.6)[44]. The mutation sites were visualized, and protein surface electrostatic potential analysis was conducted using PyMOL software.

Results

Gene structure and phylogenetic relationships of the *GS, GOGAT,* and *GDH* gene in the *Lycium* species

Both the *Lycium* species and tomato genomes or transcriptomes contain two *GOGAT* genes, namely *Fd-GOGAT* and *NADH-GOGAT*, which are 1:1 orthologous genes between *Lycium* and tomato (Fig. 1). The exon/intron structures of the *Fd-GOGAT* and *NADH-GOGAT* genes in *Lycium* and tomato consist of 33/32 and 23/22 exons/introns, respectively. Notably, the full lengths of the *Fd-GOGAT* and *NADH-GOGAT* genes are approximately 70 Kb and 12 Kb, with coding sequences (CDS) of approximately 5.0 Kb and 6.6 Kb, respectively. This suggests that *Fd-GOGAT* may possess a more complex regulatory pattern. The *Fd-GOGAT* and *NADH-GOGAT* genes in *Lycium* and tomato contain a total of 71 motifs. The number and relative positions of these motifs are nearly identical across different gene isoforms, indicating that the evolutionary trajectory of *Fd-GOGAT* and *NADH-GOGAT* proteins may be relatively conserved. However, in terms of motif quantity, the functional complexity of *NADH-GOGAT* proteins may be greater.

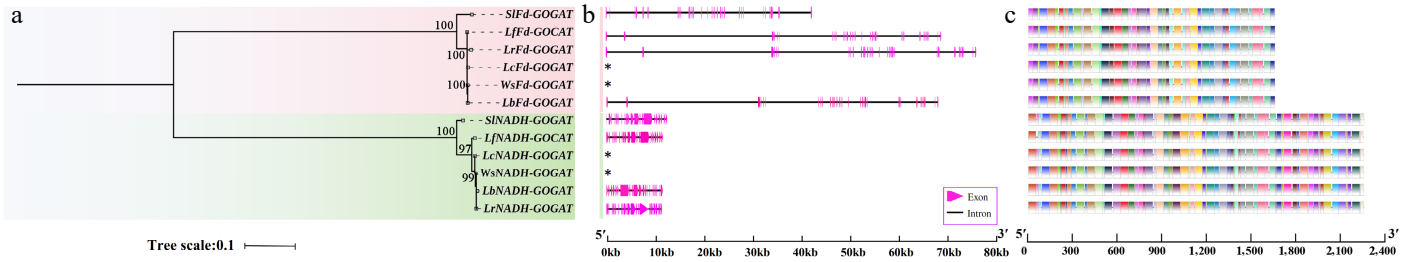

Fig. 1 Phylogenetic tree, gene structure, and motifs of the *GOGAT* genes in *Lycium* species. (a) Phylogenetic tree. (b) Gene structure. (c) Motif distribution diagram. See the legend within the figure for details.

In this study, a total of 22 *GS* genes were identified in *Lycium* species and tomato (Fig. 2). Phylogenetic analysis revealed that these genes belong to two distinct clades: the GS2 and *GS1* clades. Interestingly, *GS2* genes are single-copy genes in both *Lycium* species and tomato, whereas the number of *GS1* gene copies varies among these species. The tomato genome contains four *GS1* genes, while *Lycium* species have 1–3 *GS1* genes. For example, *L. barbarum* has only one *GS1* gene, and *L. chinense* has two, indicating that the evolution of *GS1* genes in *Lycium* species is not entirely uniform. Motif analysis showed that *GS* genes in *Lycium* species contain 14 motifs, with motif9/14 and 12 being unique to *GS2*, while the other 11 motifs are shared between *GS1* and *GS2*, possibly representing the major functional domains of *GS* genes. Gene structure analysis revealed that *GS1* genes in *Lycium* species have a structure consisting of 12 exons and 11 introns, while *GS2* genes have 13 exons and 12 introns. Moreover, the gene lengths of orthologous genes are similar, suggesting that the structural evolution of *GS* genes in *Lycium* species is highly conserved.

In this study, a total of 22 *GDH* genes were identified in *Lycium* species and tomato (Fig. 3). The phylogenetic tree revealed that these genes belong to three distinct clades: *NADP-GDH*, *GDH4*, and *GDH1/2/3* clades. *NADP-GDH* and *GDH4* are 1:1 orthologous genes in both tomato and *Lycium* species, indicating highly conserved evolution. Notably, in clade III *(GDH1/2/3*), tomato has three genes (*GDH1/2/3*), but no ortholog of tomato *GDH1* was found in *Lycium* species. Additionally, only *L. ruthenicum* and *L. barbarum* contain both *GDH2* and *GDH3*, whereas other *Lycium* species have only a single *GDH2* or *GDH3* gene in their genomes. Motif analysis showed that *GDH* genes in *Lycium* species contain 24 motifs, with *NADP-GDH* having 23 motifs, *GDH4* having 11 motifs, and *GDH2/3* having 12 motifs, with Motif20 being specific to *GDH2/3*. Gene structure analysis revealed that the gene structures of *GDH2/3/4* in *Lycium* species consist of nine exons and eight introns, while *NADP-GDH* has a structure of 15 exons and 14 introns. Interestingly, the gene lengths of *GDH* in *Lycium* species vary significantly between different species, especially for *NADP-GDH*. For example, *LfNADP-GDH* is longer than *LbNADP-GDH*. Furthermore, the gene structure of tomato *SlNADP-GDH* was found to consist of 16 exons and 15 introns, indicating that the evolution of *NADP-GDH* in *Lycium* or Solanaceae species is relatively active.

Biophysical and biochemical properties of GS, GOGAT, and GDH proteins in the *Lycium* genus

The biophysical and chemical properties of the GOGAT, GS and GDH proteins are presented in Table 1. The *Lycium* species *Fd-GOGAT* gene encodes 1,621–1,623 amino acids, with a molecular weight ranging between 176,704.76 and 176,983.22. The NADH-*GOGAT* gene encodes 2,205–2,208 amino acids, with a molecular weight ranging from 241,521.06 to 243,143.78. The grand average of hydropathy (GRAVY) values for GOGAT proteins in *Lycium* species are all less than 1, indicating that they are hydrophilic proteins.

Table 1. Biophysicochemical properties of GOGAT proteins in the *Lycium* genus.

Polypeptide chain	No. of amino acids	Molecular weight (Da)	pI	GRAVY	Instability index
LrFd-GOGAT	1,623	176,983.22	6.25	−0.15	38.04
LbFd-GOGAT	1,623	176,889.00	6.20	−0.16	38.09
LcFd-GOGAT	1,621	176,704.76	6.11	−0.16	37.80
WfFd-GOGAT	1,623	176,889.00	6.20	−0.16	38.09
LfFd-GOGAT	1,623	176,874.97	6.20	−0.16	38.42
LrNADH-GOGAT	2,208	243,143.78	6.35	−0.28	35.69
LbNADH-GOGAT	2,208	241,918.47	6.31	−0.27	35.85
LcNADH-GOGAT	2,208	241,933.38	6.31	−0.28	35.77
LfNADH-GOGAT	2,205	241,521.06	6.34	−0.28	35.21
WfNADH-GOGAT	2,208	241,913.43	6.34	−0.28	35.85
LbGDH4	411	44,519.79	6.09	−0.16	21.28
LcGDH4	411	44,461.75	6.23	−0.15	20.21
LfGDH4	411	44,504.78	6.23	−0.16	20.21
WfGDH4	411	44,505.76	6.09	−0.16	20.21
LrGDH4	411	44,505.76	6.09	−0.16	20.21
LbNADP-GDH	634	70,618.20	6.65	−0.43	36.73
LfNADP-GDH	634	70,473.98	6.65	−0.43	36.80
LcNADP-GDH	634	70,618.20	6.65	−0.43	36.73
WfNADP-GDH	634	70,634.26	6.65	−0.43	36.30
LrNADP-GDH	634	70,537.10	6.65	−0.43	37.83
LbGDH2	411	44,872.37	6.51	−0.19	20.26
LfGDH2	411	44,886.40	6.51	−0.19	21.51
LcGDH2	411	44,696.36	6.90	−0.15	21.85
WfGDH2	411	44,814.42	8.07	−0.20	21.41
LrGDH2	411	44,755.46	7.65	−0.15	22.13
LrGDH3	411	44,862.38	6.64	−0.19	19.86
LbGDH3	411	44,563.22	7.21	−0.13	21.25
LfGS2	432	47,523.80	6.12	−0.38	42.33
LbGS2	432	47,536.88	6.48	−0.38	42.06
LrGS2	432	47,564.89	6.28	−0.38	42.79
WfGS2	432	47,564.94	6.48	−0.37	42.06
LcGS2	432	47,549.92	6.73	−0.37	40.96
WfGS1.1	356	38,962.82	5.51	−0.44	37.46
LcGS1.1	356	39,160.12	5.65	−0.45	41.05
LrGS1.1	356	39,076.99	5.65	−0.45	39.67
LfGS1.1	356	39,061.03	5.65	−0.44	38.92
LbGS1.1	356	39,161.11	5.53	−0.45	41.13
LrGS1.2	356	39,076.99	5.65	−0.45	39.67
LfGS1.2	356	39,001.00	5.65	−0.40	38.53
LbGS1.2	356	39,005.03	5.79	−0.40	38.10
LbGS1.3	356	38,958.82	5.50	−0.43	37.77
LfGS1.3	356	39,003.82	5.50	−0.46	38.54
LrGS1.3	356	38,972.89	5.61	−0.43	37.46
LcGS1.3	356	39,005.03	5.79	−0.40	38.10

However, the hydrophilicity of NADH-GOGAT proteins is generally greater than that of Fd-GOGAT. Additionally, the instability index of GOGAT proteins in *Lycium* species is greater than 30, suggesting relatively low stability. Nevertheless, NADH-GOGAT exhibits slightly higher stability compared to Fd-GOGAT. Notably, the pI of the

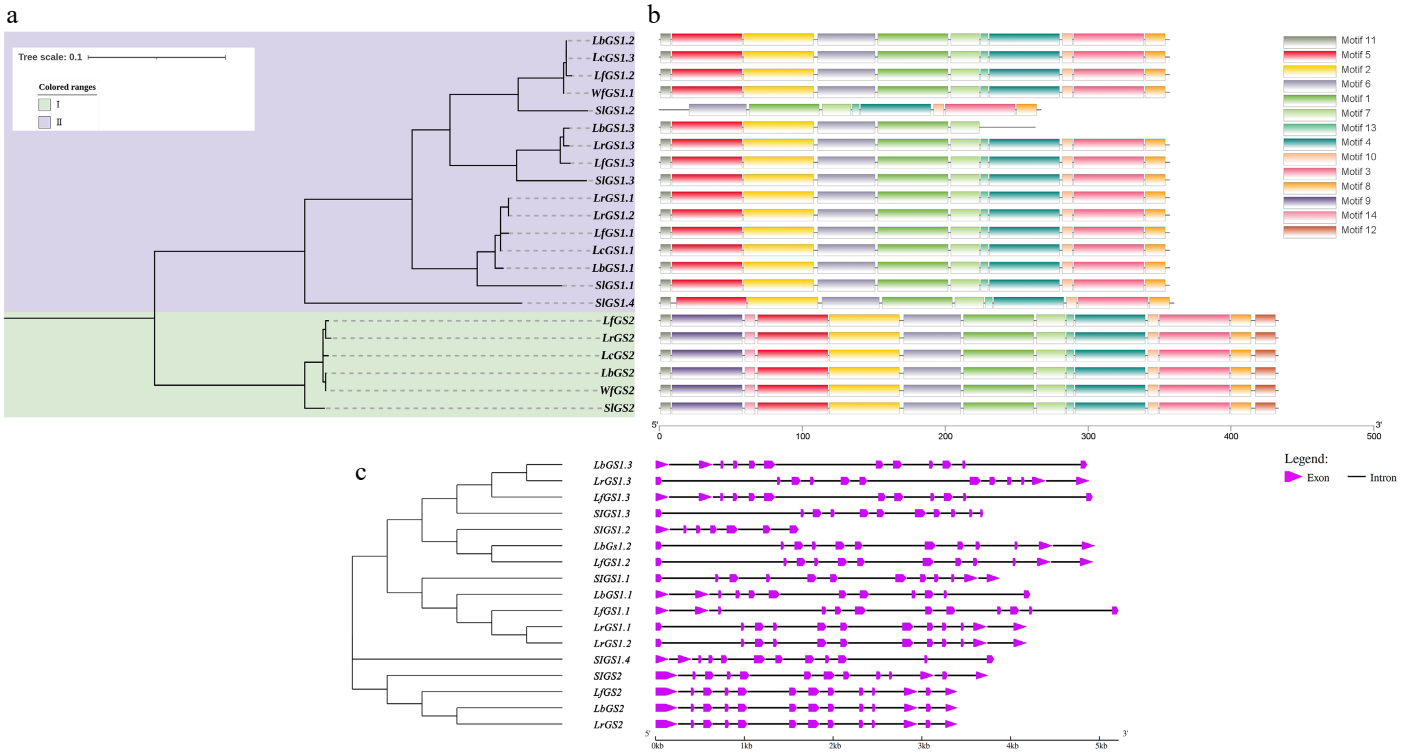

Fig. 2 Phylogenetic tree, gene structure, and motifs of the *GS* genes in *Lycium* species. (a) Represents the phylogenetic tree. (b) Depicts the motif distribution diagram. (c) Illustrates the gene structure.

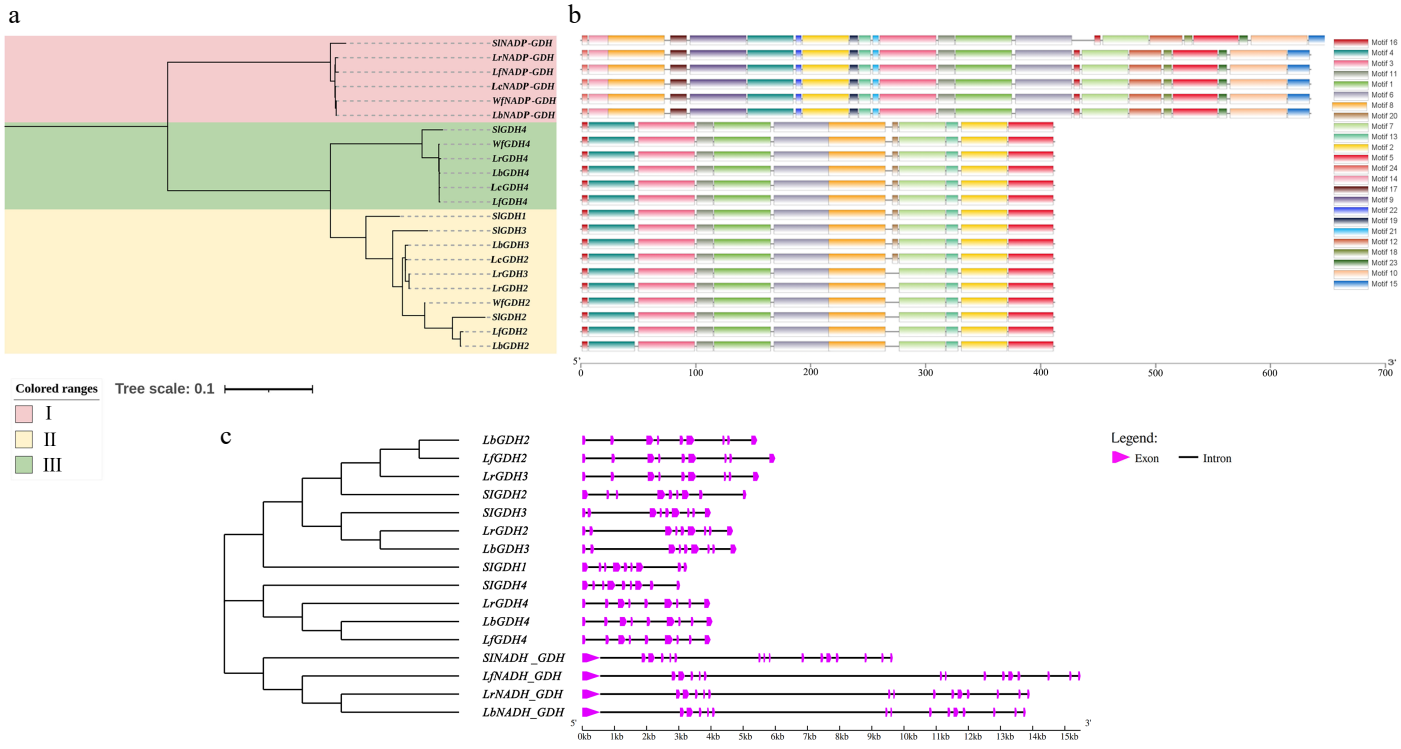

Fig. 3 Phylogenetic tree, gene structure, and motifs of the *GDH* genes in *Lycium* species. (a) Phylogenetic tree. (b) Motif distribution diagram. (c) Gene structure.

Fd/NADH-GOGAT proteins in black wolfberry is higher than that of their homologous proteins in other species. The *GS* genes encode proteins consisting of 456 or 432 amino acids, with a molecular weight ranging from 39,076.99 to 47,564.94. Overall, the pI of GS2 is > 6, while the pI of GS1 is between five and six. Compared to GS2, GS1 is more hydrophilic, as the overall GRAVY score of GS1 is less than –0.4, whereas the GRAVY score of GS2 is greater than 0.4. Additionally, all GS proteins are unstable (Instability index > 30), but GS1

is more stable than GS2. The *GDH* genes encode proteins consisting of 411 or 634 amino acids, with a molecular weight ranging from 44,755.46 to 70,634.26. The pI of GDH ranges from 6.09–8.07, and the pI of most GDH2/3 proteins is > 7. The GRAVY results indicate that all GDH proteins are hydrophilic, but NADP-GDH is significantly more hydrophilic than other GDH proteins. However, NADP-GDH is less stable (Instability index > 30), while other GDH proteins are considered stable.

Transcriptional regulation of GOGAT under salt stress in *L. ruthenicum*

Expression level of GOGAT gene under salt stress in L. ruthenicum

The results of the expression analysis (Fig. 4) show that under NaCl stress, the expression level of *LrFd-GOGAT* in leaf tissues was significantly downregulated. Specifically, under 0.5% NaCl treatment, the expression was reduced by 21% and 32% at 1 and 12 h, respectively. Although the expression level was upregulated under 0.5% NaCl treatment, there was no significant difference compared to CK. Furthermore, with the prolongation of time after treatment, the expression of *LrFd-GOGAT* in leaf tissues was markedly downregulated. In contrast, under NaCl stress, the expression of *LrFd-GOGAT* in root tissues was mainly upregulated, particularly at 12 h after NaCl treatment, where it was upregulated by 1.79-fold under 2.5% NaCl treatment.The expression pattern of *LrNADH-GOGAT* in leaf tissues was similar to that of *LrFd-GOGAT*. It is noteworthy that the inhibitory effect on *LrNADH-GOGAT* was more severe. In root tissues, the expression of *LrNADH-GOGAT* showed no significant change under 0.5% NaCl treatment. However, under 2.5% NaCl treatment, its expression was significantly downregulated at 1 h compared to CK, but was significantly upregulated at 12 h, reaching 1.40-fold of the control.

The expression levels of *LrGSs* under salt stress are shown in Fig. 5. *LrGS2* is the predominantly expressed *GS* gene in leaves (Fig. 5c). The expression of *LrGS2* in leaves was significantly upregulated after 1 h of 2.5% NaCl stress, and although its expression level decreased by 12 h of stress, it did not fall below the normal physiological level. This indicates that *LrGS2* can be induced by salt stress but that salt stress does not suppress its expression level in leaves. The expression of *LrGS2* in roots was low, but it was significantly upregulated after 1 h of 0.5% NaCl stress (Fig. 5g). In addition, the expression level of *LrGS1.2* in leaves was also significantly upregulated after 1 h of 0.5% NaCl stress (Fig. 5d). *LrGS1.1* is the predominantly expressed *GS* gene in roots, and its expression was upregulated by 1.59-fold after 1 h of 0.5% NaCl stress (Fig. 5e). As the degree of stress increased and the duration of stress continued, the expression of *LrGS1.1* was significantly downregulated. Furthermore, with increasing salt concentration and prolonged stress duration, the expression levels of other *GS* genes were also downregulated, both in leaves and roots.

The expression levels of *LrGDHs* are much lower than those of *LrGSs* (Fig. 6), and the expression levels of most *LrGSs* genes decreased under NaCl stress, especially in leaves. *LrGDH4* is the predominantly expressed *GDH* gene in both leaves and roots, and its expression was significantly downregulated in both roots and leaves under NaCl stress. However, it is noteworthy that the expression levels of *LrNADP-GDH* and *LrGDH2* were significantly upregulated at 12 h of NaCl stress.

Transcriptional regulatory network of the GOGAT gene in L. ruthenicum

The protein-protein interaction results showed that out of the ten nitrogen assimilation-related genes in black wolfberry, seven exhibited significant interactions, including two GOGAT, two GS, and

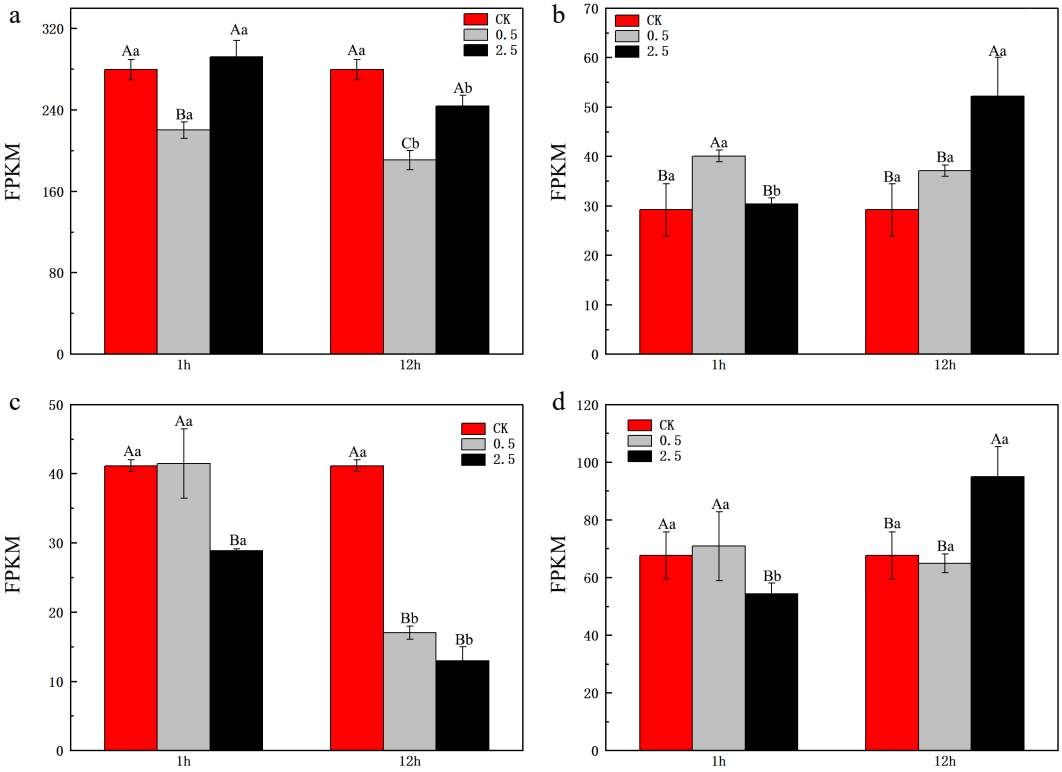

Fig. 4 Expression levels of *GOGAT* in the leaves and roots of *L. ruthenicum* under NaCl treatment. (a) Expression level of *LrFd-GOGAT* in leaf tissues. (b) Expression level of *LrFd-GOGAT* in root tissues. (c) Expression level of *LrNADH-GOGAT* in leaf tissues. (d) Expression level of *LrNADH-GOGAT* in root tissues. Different uppercase letters (A, B, C) within the same subfigure indicate statistically significant differences ($p < 0.05$) among samples within a group, while distinct lowercase letters (a, b, c) represent significant differences ($p < 0.05$) between different groups.

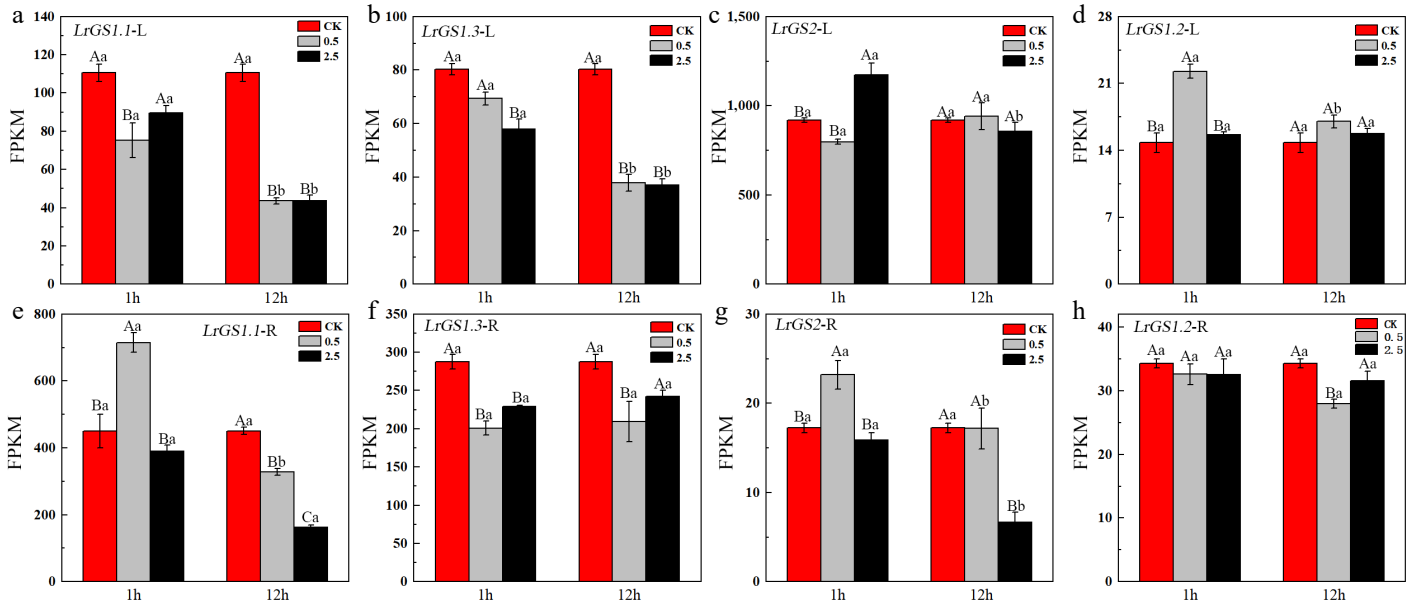

Fig. 5 Expression levels of *GS* in the leaves and roots of *L. ruthenicum* under NaCl treatment. Different uppercase letters (A, B, C) within the same subfigure indicate statistically significant differences ($p < 0.05$) among samples within a group, while distinct lowercase letters (a, b, c) represent significant differences ($p < 0.05$) between different groups. 'L' is leaf, 'R' is root.

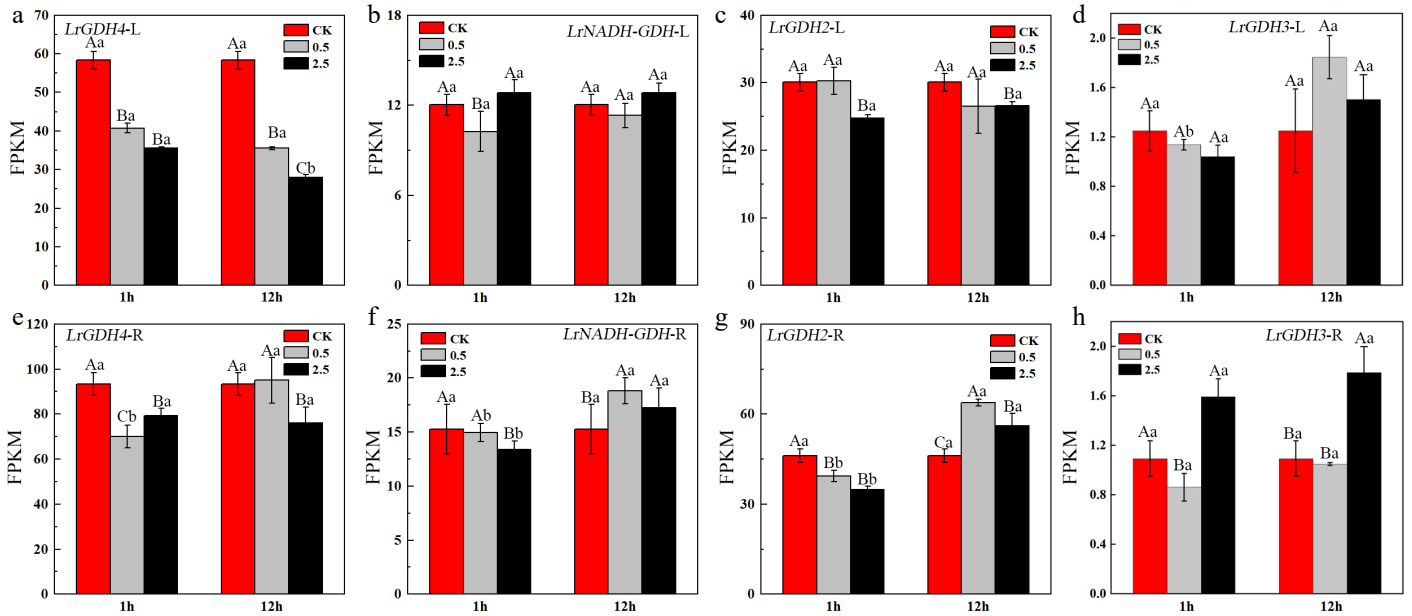

Fig. 6 Expression levels of GDH in the leaves and roots of *L. ruthenicum* under NaCl treatment. Different uppercase letters (A, B, C) within the same subfigure indicate statistically significant differences ($p < 0.05$) among samples within a group, while distinct lowercase letters (a, b, c) represent significant differences ($p < 0.05$) between different groups. 'L' is leaf, 'R' is root.

two GDH (Fig. 7a). To explore the role of transcription factors (TFs) in the regulation of nitrogen assimilation in black wolfberry, transcription factors regulating the expression of nitrogen assimilation-related genes were predicted. The results indicated that 19 TF families may be involved in the regulation of the seven nitrogen assimilation-related genes in black wolfberry, with the C2H2, Dof, GRAS, AP2, and BBR-BPC families having the highest number of binding sites (Fig. 7b). Therefore, members of these five TF families were identified and their expression under salt stress was analyzed. The results showed that 42 *AP2* genes, six *BBR-BPC* genes, 84 *C2H2* genes, 36 *Dof* genes, and 20 *GRAS* genes were expressed in the leaves and roots of black wolfberry. Under salt stress, their expression patterns in leaves and roots were classified into eight distinct expression profiles (Fig. 7c, d). In the leaves, the expression levels of 13 genes were upregulated with increasing salt stress concentration and duration. In the roots, the expression levels of four genes were upregulated with increasing salt stress concentration and duration. Notably, *C2H2-63* was the only gene whose expression level in both roots and leaves was upregulated with increasing salt concentration and stress duration.The expression analysis of *C2H2-63* showed that under normal physiological conditions, the expression level of *C2H2-63* in roots was 3.6 times higher than in leaves. Under 0.5% NaCl stress, there was no significant change in the expression levels of *C2H2-63* in roots and leaves. However, under 2.5% NaCl stress, the expression of *C2H2-63* was upregulated by 2.33-fold and 2.15-fold after 1 h and 12 h of stress in roots,

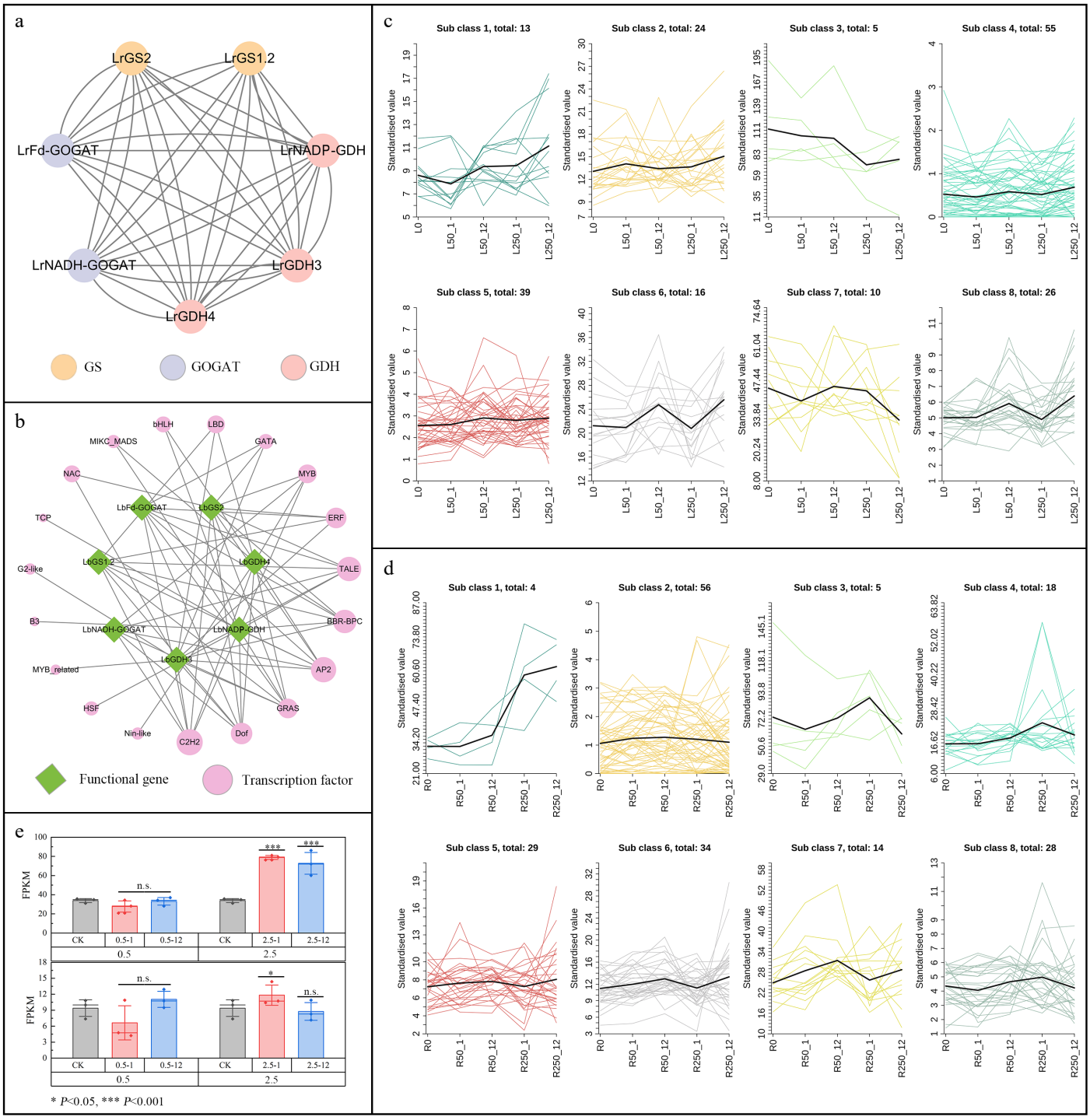

Fig. 7 Transcription regulatory network and correlation analysis of *GOGAT*, *GS*, and *GDH* in *L. ruthenicum*. (a) Protein interaction networks of GOGAT, GS, and GDH. (b) Transcription factor regulatory network for protein interaction. (c) Expression pattern of TFs under salt stress in leaves. (d) Expression pattern of TFs under salt stress in root. (e) Expression of C2H2-63 under salt stress.

respectively, and by 1.30-fold after 1 h of stress in leaves. This suggests that *C2H2-63* plays a positive role in the response of black wolfberry to salt stress.

TF-DNA docking analysis

To verify whether C2H2-63 has a regulatory role in the nitrogen assimilation-related genes of black wolfberry, this study used AF3 to perform molecular docking of C2H2-63 with the promoter regions of the seven nitrogen assimilation-related genes. The results showed that the C2H2-63 protein structure contains a typical C2H2 domain (Fig. 8a), and that C2H2-63 is able to bind to the promoter regions of all seven nitrogen assimilation-related genes in black wolfberry (Fig. 8b–h).

Molecular evolution analysis and comparative protein structure analysis

Selective pressure on GOGAT, GS, and GDH genes and sites of positive selection

To test whether the proteins encoded by the *GOGAT*, *GS*, and *GDH* genes in black wolfberry are subject to positive selection at specific

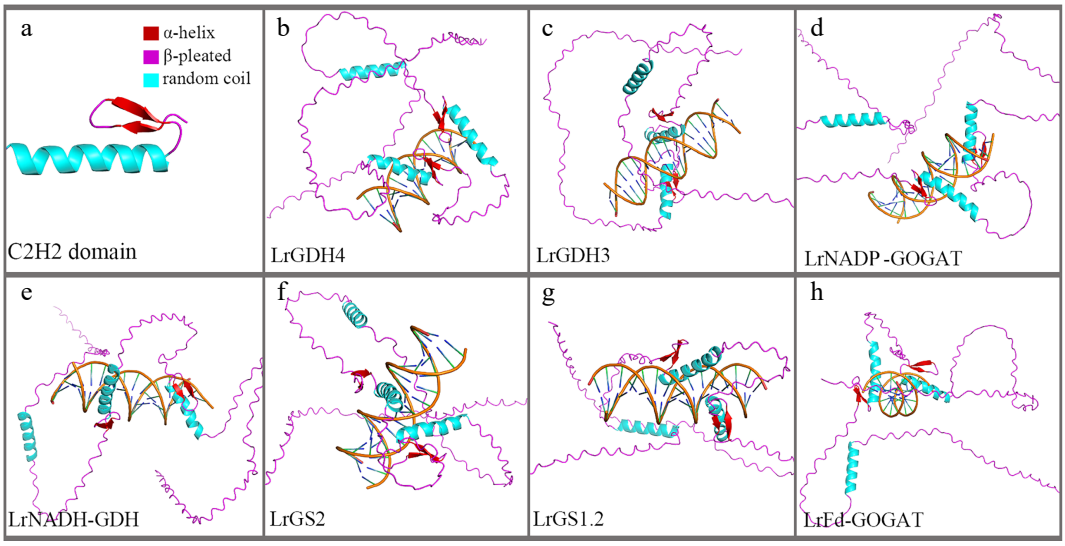

Fig. 8 TF-DNA docking diagram. (a) Tertiary structure of the C2H2 domain. (b)–(h) Binding conformations with promoter regions of different genes.

amino acid sites, the branch-site model was employed for analysis. The results (Supplementary Fig. S1) revealed that the amino acid sites p.Glu223Ala, p.Ala391Phe, p.Ala883Thr, p.Ser924Leu, p.Leu1322Phe, p.Ser1353Ala, and p.Ser1573Cys in the *Fd-GOGAT* gene of black wolfberry are under strong positive selection. LRT results indicated a significant difference between Model A0 and Model A1 ($p < 0.05$) (Table 2).

Construction and quality assessment of protein structure models

To investigate whether mutation sites affect the structure and function of the LrFd-GOGAT protein, this study constructed the three-dimensional structures of LrFd-GOGAT and LbFd-GOGAT proteins. The results, as illustrated in Fig. 9a, reveal that both LrFd-GOGAT and LbFd-GOGAT are monomeric proteins composed of four distinct domains and two ligands. The domains include the FMN-binding domain, C-terminal domain, central domain, and N-terminal amidotransferase domain. The ligands are 3Fe-4S and FMN. In the LrFd-GOGAT protein, seven mutation sites were identified: p.Ser924Leu and p.Leu1322Phe are located within the FMN-binding domain; p.Ser1353Ala and p.Ser1573Cys reside in the C-terminal domain; p.Glu223Ala and p.Ala391Phe are found in the amidotransferase domain; and p.Ala880Thr is situated in the central domain (Fig. 9b). The Ramachandran plot shows that 91.2% and 92.6% of the amino acid residues of LrFd-GOGAT and LbFd-GOGAT (Supplementary Fig. S2), respectively, fall within the red regions, indicating a high quality of the protein models, which allows for reliable structural comparison and analysis.

Comparative analysis of protein structures

To explore the differences in structure and function between LrFd-GOGAT and LbFd-GOGAT, this study conducted a point mutation analysis of LbFd-GOGAT, specifically targeting the positively selected sites of LrFd-GOGAT. The results showed that the Root Mean Square Deviation (RMSD) between LrFd-GOGAT and LbFd-GOGAT was 0.121, indicating that the mutation sites did not cause significant changes in the overall protein structure of LrFd-GOGAT. Further analysis revealed that the mutation p.Leu1322Phe altered the original unstructured coil region, introducing an additional helical structure between Phe1322 and Ser1327 in the LrFd-GOGAT protein (Fig. 10). No other structural changes caused by mutation sites were observed.

However, it is noteworthy that both p.Glu223Ala and p.Ala391Phe are located in the amidotransferase domain. The analysis indicated that these two mutations increased the electrostatic potential in the corresponding regions (on the protein surface), while other mutation sites did not alter the electrostatic potential of their respective regions (Fig. 11).

Additionally, the impact of mutation sites on protein hydrophilicity was analyzed. The mutations p.Ala883Thr and p.Leu1322Phe led to an increase in hydrophilicity in the respective regions, whereas p.Glu223Ala, p.Ala391Phe, p.Ser924Leu, p.Ser1353Ala, and p.Ser1573Cys resulted in increased hydrophobicity in their corresponding regions (Fig. 12). Notably, p.Ala883Thr and p.Leu1322Phe are both located in unstructured coil regions, while p.Glu223Ala, p.Ala391Phe, p.Ser924Leu, p.Ser1353Ala, and p.Ser1573Cys are all situated in helical structures.

Molecular docking

To analyze whether the mutation sites would lead to a change in the binding affinity of LrFd-GOGAT with its substrate, this study conducted molecular docking simulations between LrFd-GOGAT and LbFd-GOGAT with the substrate L-glutamine. After performing 50 rounds of docking simulations, it was found that both LrFd-GOGAT and LbFd-GOGAT had ten potential binding sites with L-glutamine, among which two sites exhibited binding energies greater than |–2 kJ/mol| in both LrFd-GOGAT and LbFd-GOGAT (Fig. 13). A comparative analysis revealed that the binding energies of LrFd-GOGAT with L-glutamine were –2.99 kJ/mol and –2.96 kJ/mol, respectively, while the binding energies of LbFd-GOGAT with L-glutamine were –2.90 kJ/mol and –2.36 kJ/mol, respectively. This indicates that LrFd-GOGAT has a higher affinity for the substrate L-glutamine.

Discussion

Evolution of *GS*, *GOGAT*, and *GDH* genes in *Lycium* species

Given the crucial role of nitrogen assimilation in plant growth, *GS*, *GOGAT*, and *GDH* genes from numerous species have been identified and functionally characterized. Currently, two types of GOGAT proteins, Fd-GOGAT and NADH-GOGAT, have been found in most higher plants[45–48]. However, the number of GOGAT-encoding genes varies significantly across different plant lineages. For instance, the genomes of tomato[49] and pine *(Pinus taeda)*[50] each contain one *Fd-GOGAT* gene and one *NADH-GOGAT* gene; the rice

Table 2. Molecular evolutionary analysis based on the branch-site model.

Gene	Mode	Estimates of parameters	NP	lnL	χ^2	df	*p*
LrFd-GOGAT	Model A0	Proportion 0.79 0.07 0.13 0.01					
		Background w 0.00 1.00 0.00 1.00	11	−6783.17		Model A0 vs Model A1	
		Foreground w 0.00 1.00 1.00 1.00			6.2	1	0.01
	Model A1	Proportion 0.99 0.00 0.01 0.00					
		Background w 0.07 1.00 0.07 1.00	12	−6780.07			
		Foreground w 0.07 1.00 65.77 65.77					
LrNADH-GOGAT	Model A0	Proportion 0.90 0.10 0.00 0.00					
		Background w 0.00 1.00 0.00 1.00	15	−9501.4		Model A0 vs Model A1	
		Foreground w 0.00 1.00 1.00 1.00			0	1	1
	Model A1	Proportion 0.90 0.10 0.00 0.00					
		Background w 0.00 1.00 0.00 1.00	16	−9501.4			
		Foreground w 0.00 1.00 1.00 1.00					
LrGDH2	Model A0	Proportion 0.82 0.07 0.10 0.01					
		Background w 0.05 1.00 0.05 1.00	15	−2448.84		Model A0 vs Model A1	
		Foreground w 0.05 1.00 1.00 1.00			0	1	1
	Model A1	Proportion 0.90 0.08 0.02 0.00					
		Background w 0.05 1.00 0.05 1.00	16	−2448.84			
		Foreground w 0.05 1.00 1.00 1.00					
LrGDH3	Model A0	Proportion 0.92 0.08 0.00 0.00					
		Background w 0.05 1.00 0.05 1.00	15	−2,889.45		Model A0 vs Model A1	
		Foreground w 0.05 1.00 1.00 1.00			0	1	1
	Model A1	Proportion 0.91 0.08 0.01 0.00					
		Background w 0.05 1.00 0.04 1.00	16	−2889.45			
		Foreground w 0.05 1.00 1.00 1.00					
LrNADP-GDH	Model A0	Proportion 0.85 0.15 0.00 0.00					
		Background w 0.00 1.00 0.00 1.00	11	−2755.77		Model A0 vs Model A1	
		Foreground w 0.00 1.00 1.00 1.00			0	1	1
	Model A1	Proportion 0.85 0.15 0.00 0.00					
		Background w 0.00 1.00 0.00 1.00	12	−2755.77			
		Foreground w 0.00 1.00 1.00 1.00					
LrGDH4	Model A0	Proportion 0.93 0.07 0.00 0.00					
		Background w 0.00 1.00 0.00 1.00	11	−1713.21		Model A0 vs Model A1	
		Foreground w 0.00 1.00 1.00 1.00			0	1	1
	Model A1	Proportion 0.93 0.07 0.00 0.00					
		Background w 0.00 1.00 0.00 1.00	12	−1713.21			
		Foreground w 0.00 1.00 1.00 1.00					
LrGS1.1	Model A0	Proportion 0.74 0.03 0.22 0.01					
		Background w 0.06 1.00 0.06 1.00	11	−2013.92		Model A0 vs Model A1	
		Foreground w 0.56 1.00 1.00 1.00			0	1	1
	Model A1	Proportion 0.79 0.03 0.17 0.01					
		Background w 0.06 1.00 0.06 1.00	12	−2013.91			
		Foreground w 0.06 1.00 1.31 1.31					
LrGS2	Model A0	Proportion 0.77 0.16 0.06 0.01					
		Background w 0.00 1.00 0.00 1.00	11	−1870.56		Model A0 vs Model A1	
		Foreground w 0.00 1.00 1.00 1.00			0	1	1
	Model A1	Proportion 0.77 0.16 0.06 0.01					
		Background w 0.00 1.00 0.00 1.00	12	−1870.56			
		Foreground w 0.00 1.00 1.00 1.00					
LrGS1.2	Model A0	Proportion 0.89 0.07 0.04 0.00					
		Background w 0.04 1.00 0.04 1.00	15	−2473.48		Model A0 vs Model A1	
		Foreground w 0.04 1.00 1.00 1.00			0	1	1
	Model A1	Proportion 0.89 0.07 0.04 0.00					
		Background w 0.04 1.00 0.04 1.00	16	−2473.48			
		Foreground w 0.04 1.00 1.00 1.00					
LrGS1.3	Model A0	Proportion 0.92 0.07 0.00 0.00					
		Background w 0.04 1.00 0.04 1.00	15	−2474.1		Model A0 vs Model A1	
		Foreground w 0.04 1.00 1.00 1.00			0	1	1
	Model A1	Proportion 0.93 0.07 0.00 0.00					
		Background w 0.04 1.00 0.04 1.00	16	−2474.1			
		Foreground w 0.04 1.00 1.00 1.00					

genome[51] has two genes encoding NADH-GOGAT proteins and one gene encoding Fd-GOGAT; the genomes of *Populus trichocarpa*[52] and *Carya illinoinensis*[53] each contain four *GOGAT* genes, with two encoding Fd-GOGAT proteins and two encoding NADH-GOGAT proteins; and the wheat genome contains six *GOGAT* genes, with three encoding Fd-GOGAT proteins and three encoding NADH-GOGAT proteins[54]. This study identified two *GOGAT* genes in both *L. ruthenicum* and tomato genomes, each encoding one

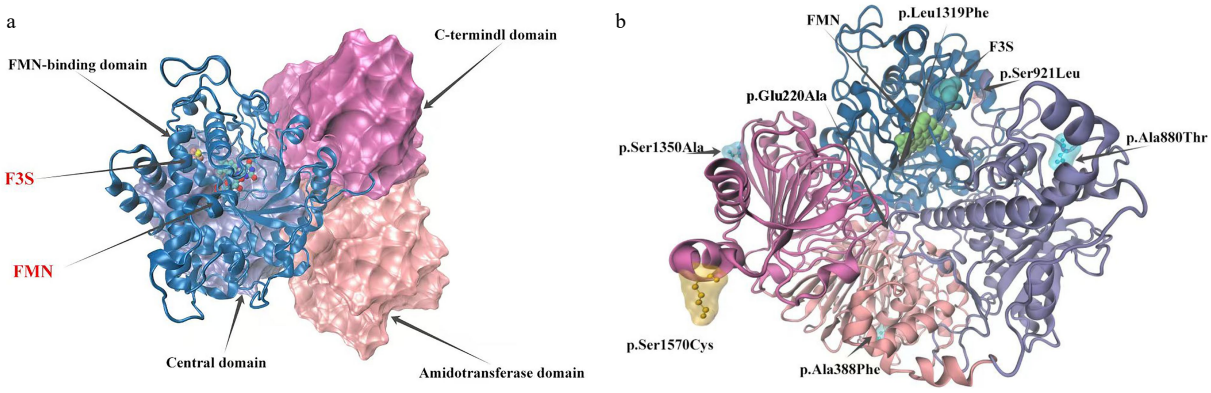

Fig. 9 Model of LrFd-GOGAT protein structure and distribution of mutation sites. (a) Structural model of the LrFd-GOGAT protein. (b) Distribution of amino acid mutation sites in the LrFd-GOGAT protein.

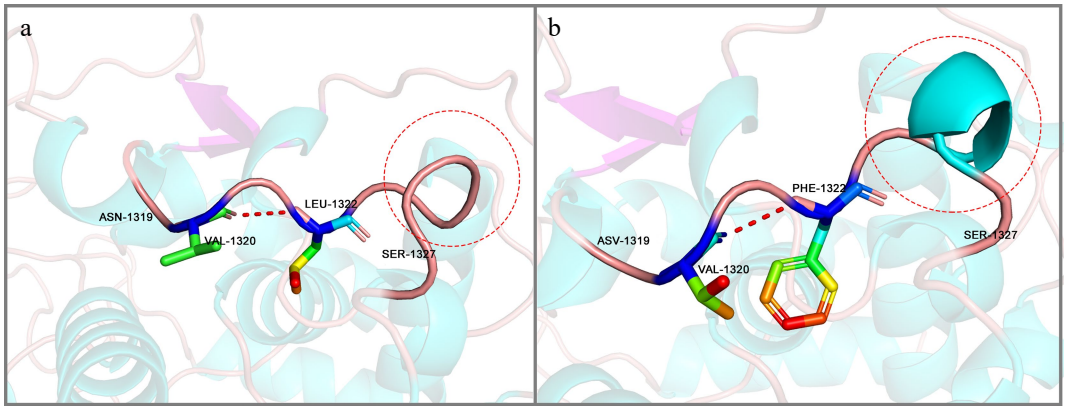

Fig. 10 Protein conformation at the p.Leu1322Phe position. (a) Conformational structure of the Leu 1322 region in LbFd-GOGAT. (b) Corresponding Phe1322 region conformation in LrFd-GOGAT.

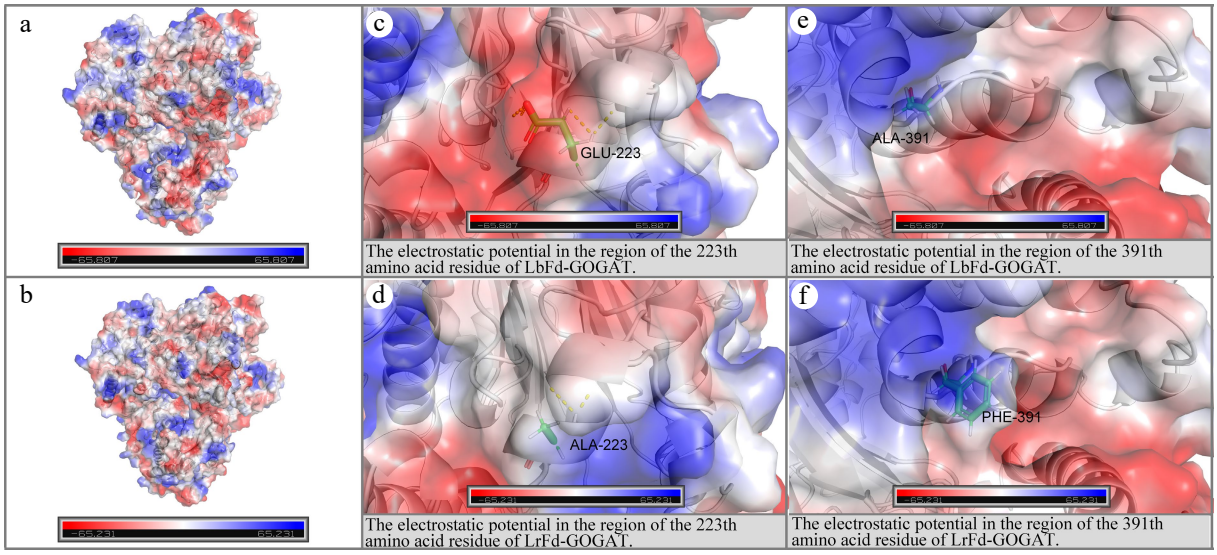

Fig. 11 Electrostatic potential distribution in the regions of p.Glu223Ala and p.Ala391Phe. (a) and (b) depict the electrostatic potential distributions on the molecular surfaces of LbFd-GOGAT and LrFd-GOGAT proteins, respectively; (c) and (d) present the localized electrostatic potential distributions surrounding residue 223 in LbFd-GOGAT and LrFd-GOGAT proteins; (e) and (f) illustrate the electrostatic potential profiles near residue 391 in LbFd-GOGAT and LrFd-GOGAT proteins.

Fd-GOGAT and one NADH-GOGAT protein. These findings suggest that *GOGAT* genes may have undergone duplication, loss, or functional divergence during the evolution of different plant lineages. However, the evolution of *GOGAT* genes in *Lycium* species or Solanaceae appears to be relatively stable, potentially indicating a consistent key role in nitrogen assimilation. Tomato and pine *Fd-GOGAT* genes contain 33 exons[49,50]. The results in this study are consistent with this, as *Lycium* species' *Fd-GOGAT* genes also contain 33 exons. However, the intron lengths in *Lycium* species' *Fd-GOGAT* genes are significantly longer than those in tomato, a phenomenon

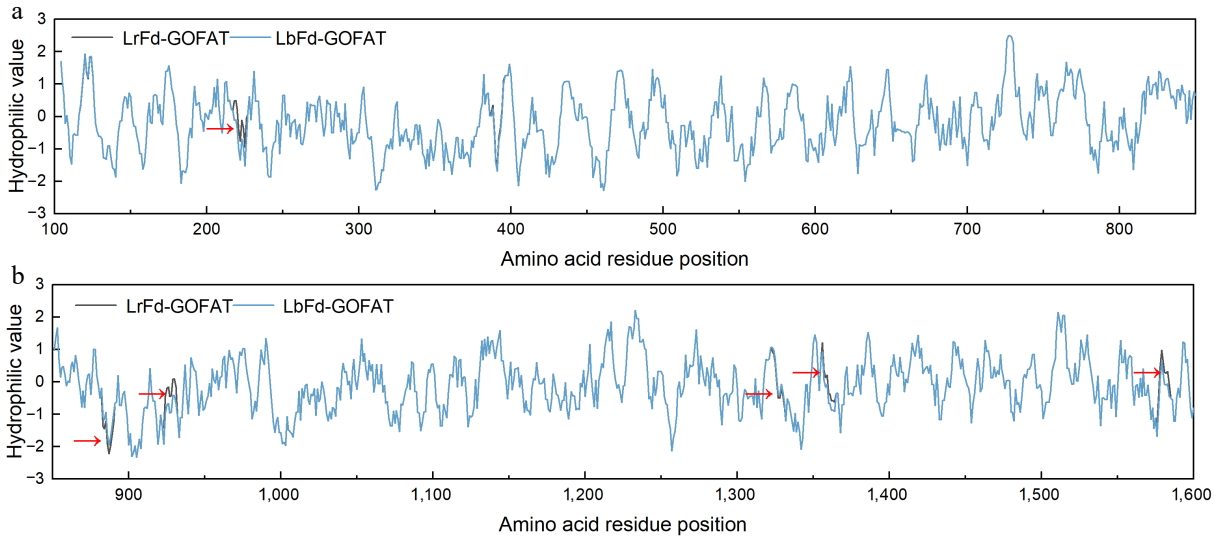

Fig. 12 Hydrophilicity distribution of amino acid residues in LrFd-GOGAT and LbFd-GOGAT proteins. (a) and (b) display the hydrophilicity profiles of amino acid residues 100–850 and 851–1,600, respectively.

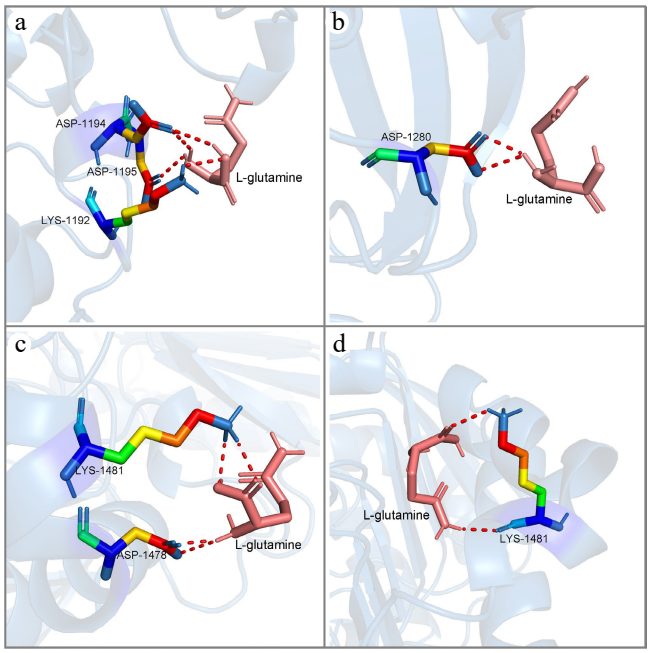

Fig. 13 The molecular conformations of LrFd-GOGAT and LbFd-GOGAT in docking with L-glutamine. (a) and (b) show the two lowest binding energy conformations of LbFd-GOGAT docked with L-glutamine, respectively; (c) and (d) show the two lowest binding energy conformations of LrFd-GOGAT docked with L-glutamine, respectively.

also observed in other woody plants, such as pine, where the longest *Fd-GOGAT* intron reaches 50 kb. The gene structure of *NADH-GOGAT* varies considerably between species. This study found that *Lycium* species' *NADH-GOGAT* contains 23 exons, consistent with the structure in tomato. However, *NADH-GOGAT* in other species has been found to have 22 (pine)[50] or 20 (rice, *Carya illinoinensis*)[51] exons. Notably, the intron lengths of the *NADH-GOGAT* gene are relatively conserved across most species. These results indicate that the coding regions of plant *Fd-GOGAT* genes are evolutionarily conserved, but the non-coding regions are longer in woody plants, suggesting more complex regulatory mechanisms in woody plants compared to herbaceous plants. The evolutionary strategy of *NADH-GOGAT* differs from that of *Fd-GOGAT*, mainly manifesting in significant variation in the coding regions of *NADH-GOGAT* across different lineages, which may reflect differences in protein function.

In higher plants, *GS* proteins are encoded by multiple genes, including two isoforms: *GS1* and *GS2*. However, there is considerable variation in the number of genes encoding *GS1* and *GS2* proteins among different plant lineages. In angiosperms, the number of genes encoding the *GS2* isoform is typically only one, whereas the number of genes encoding the GS1 isoform usually ranges from two to five[55–57]. In this study, it was observed that there is one gene encoding *GS2* in *Lycium* species, which is consistent with previous findings, indicating that *GS2* has evolved in a highly conserved manner in plants. Unexpectedly, one to three GS1 genes in *Lycium* species were identified, with only one *GS1* gene found in the transcriptome of white fruit *of L. ruthenicum*. This discrepancy might be related to false negatives in de novo transcriptome assembly[58], as three *GS1* genes were identified in the genomes of both *L. ferocissimum, L. ruthenicum* and *L. barbarum*. Therefore, this study speculates that the *Lycium* species genome contains three GS1 genes, and their evolution is highly conserved, as they maintain a high degree of consistency in the number of family members, gene structure, and motifs. *GDH* is present in various tissues of plants and is responsible for catalyzing the formation of Glu from α-ketoglutarate and NH_4^+[59]. Plants possess unique *GDH* isoenzymes that are specific to either NAD or NADP[60]. NAD-specific *GDH* is located in the mitochondria[61], while NADP-utilizing GDH is found in the chloroplasts[62]. In plants, *GDH* enzymes are usually homo- or heteromultimers composed of four or six subunits; thus, plants generally contain at least two *GDH* genes encoding two *GDH* polypeptide subunits. In Arabidopsis, there are three NAD-specific GDH genes and one NADP-specific GDH, namely *AtGDH1*, *AtGDH2*, *AtGDH3*, and *NADP-GDH*[63]. Five GDH genes have been identified in tomato[64], including four NAD-specific GDH genes and one NADP-specific GDH, which is consistent with the results identified in this study. In this study, four GDH genes in *Lycium* species were discovered, including one NADP-GDH and three NAD-specific GDH genes. The NADP-GDH and *GDH4* are highly conserved, but *GDH2* and *GDH3* may have been lost in some species during evolution.

The response patterns of *GS*, *GOGAT*, and *GDH* to salt stress in *L. ruthenicum*

The GS/GOGAT cycle is the primary ammonium assimilation pathway in plants. Previous studies have reported that the GS/GOGAT

cycle accounts for approximately 95% of total ammonium assimilation, whereas the GDH assimilation pathway contributes only about 5% to total ammonium assimilation. Therefore, changes in the expression levels of GS and GOGAT are crucial for NH_4^+ assimilation in plants under salt stress. Studies have found that, compared to salt-sensitive strains, salt-tolerant strains exhibit higher transcriptional levels and enzyme activity of GOGAT, as reported in various species such as soybean and wheat[17,65]. Hence, variations in GOGAT enzyme activity are often used to assess plant tolerance to salt stress in subsequent research. Numerous studies have shown that Fd-GOGAT is primarily expressed in photosynthetic tissues and is mainly responsible for assimilating NH_4^+ produced by photorespiration and NO_3^- reduction[8]. This study revealed that the *Fd-GOGAT* gene in black wolfberry is predominantly expressed in leaves, and its expression tends to be downregulated as NaCl concentrations increase and stress duration lengthens. It is well known that salt stress inhibits chlorophyll production and reduces the photosynthetic rate in green plants, leading to a significant decrease in NH_4^+ content generated by photosynthesis[66]. Since NH_4^+ is the substrate for the GS/GOGAT cycle, the reduction in its levels slows down the cycle, which may primarily account for the decreased expression of *LrFd-GOGAT* in leaves. Additionally, *LrNADH-GOGAT* is also expressed in leaves, although at much lower levels compared to *LrFd-GOGAT*, consistent with previous findings, where *NADH-GOGAT* activity constitutes only 3% of total GOGAT activity in leaves[67]. Similarly, the expression of LrNADH-GOGAT is significantly downregulated under salt stress, and compared to LrFd-GOGAT, the downregulation of LrNADH-GOGAT is more pronounced, continuously decreasing with higher salt concentrations and prolonged stress durations. Research on rice has shown that NADH-GOGAT is mainly distributed in leaf phloem tissues and plays a significant role in the transport of nitrogen compounds[68], further supporting the notion that the reduction in leaf GOGAT activity is likely due to substrate depletion. In roots, GOGAT primarily assimilates NO_3^- and NH_4^+ absorbed by the root system[69]. Excessive salinity can competitively inhibit the uptake of NO_3^- and NH_4^+ by Cl^- and Na^+, leading to reduced nitrogen uptake and decreased expression of nitrogen assimilation genes in the roots[70]. In this study, both *LrNADH-GOGAT* and *LrFd-GOGAT* were expressed in the roots, and their expression levels were significantly upregulated under severe salt stress and after 12 h of stress. This finding is inconsistent with previous studies. Apart from the GS/GOGAT pathway for inorganic nitrogen assimilation, plants also possess the GDH pathway, which has a lower affinity for NH_4^+[69,70]. Typically, under salt stress, the reduction in NH_4^+ levels and the decline in assimilation enzyme activity prompt plants to activate the GDH pathway for NH_4^+ assimilation. However, this study found that the expression of GOGAT genes in the roots of black wolfberry did not decrease but instead was upregulated. This suggests that under salt stress, the roots of black wolfberry may accelerate NH_4^+ assimilation via the GS/GOGAT pathway, an evolutionary strategy that helps maintain a substantial nitrogen supply in the roots even under extreme salt stress.

The high expression of *GS* genes is one of the primary strategies for plants to maintain NUE under salt stress. Studies in rice have shown that overexpression of *OsGS2* can significantly enhance the photosynthesis and salt tolerance of transgenic rice plants[71]. *GS2* is mainly expressed in photosynthetic tissues, assimilating NH_4^+ from nitrate reduction and photorespiration in leaves, whereas GS1 assimilates NH_4^+ from other metabolic processes[72]. This is consistent with the findings of this study, where we found that *LrGS2* is the predominantly expressed gene in leaves, and *LrGS1.1* is the predominantly expressed gene in roots. Research on most plants has shown that salt stress reduces the expression levels and enzymatic activity of *GS* genes, primarily related to nitrogen uptake under salt stress. Similar to GOGAT, salt stress leads to a decrease in the substrates available for GS activity. This study found that the expression levels of most *LrGS* genes were downregulated under salt stress, but the upregulation of *LrGS2* in leaves and *LrGS1.1* in roots was not coincidental. We observed that the upregulation of *LrGS* occurred 1 h after salt stress, while the upregulation of *LrGOGATs* occurred 12 h after exposure to 2.5% NaCl. This suggests that under salt stress, *Lycium ruthenicum* may maintain high NUE by highly expressing its major genes to alleviate the nutrient uptake deficiency caused by salt stress. Although the contribution of GDH to nitrogen assimilation in plants is minimal, it is considered to be a primary backup pathway for nitrogen assimilation under environmental stress. This is supported by multiple experiments showing that the expression levels and enzymatic activity of GDH are upregulated under salt stress[73]. In this study, it was found that the expression of *LrGDHs* was mostly downregulated under salt stress, especially in leaves, where all four GDH genes were downregulated. Notably, the expression of *NADP-GDH* and *LrGDH2* in roots was continuously upregulated with increasing salt concentration and duration of stress. These findings suggest that GDH is not the main nitrogen assimilation pathway in the leaves of *Lycium ruthenicum* under salt stress. GDH directly catalyzes the production of Glu from ammonium and 2-oxoglutarate (2-OG), and this reaction is reversible. An increase in GDH enzymatic activity may, on one hand, lead to an increase in 2-OG, which can enter the tricarboxylic acid (TCA) cycle to provide energy for plant metabolic activities[74]. On the other hand, proline, as an osmotic regulator, plays a major protective role in plants under osmotic stress. The synthesis of proline from Glu is a primary pathway selected by plants under salt stress[75]. Previous studies have shown that the proline content in the leaves and roots of *L. ruthenicum* significantly increases under salt stress, and the content in roots is significantly higher than in leaves. Therefore, the upregulation of *NADP-GDH* and *LrGDH2* in roots may be associated with increased proline synthesis in root tissues.

Transcription factors regulate the transcription of nitrogen transporters, assimilation enzymes, and signaling molecules to ensure plant nitrogen availability under adverse conditions[68]. Gaudinier et al. constructed a transcriptional regulatory network involving 21 transcription factors associated with plant nitrogen metabolism pathways and found that transcription factors from families such as C2H2(ZFP), ERF, and DOF play crucial regulatory roles in nitrogen metabolism. Specifically, *ZFP7*, *ERF070*, and *DOF1.5* are all involved in the NH_4^+ assimilation process[76]. Under nitrogen-deficient conditions, wheat can alleviate stress damage caused by low nitrogen by upregulating TaZFP593. Transgenic TaZFP593 overexpressing tobacco plants exhibit increased nitrogen accumulation under nitrogen deficiency and can upregulate *GS* activity to enhance nitrogen assimilation[77]. In nitrogen-deficient environments, the overexpression of Dof1 in maize, a transcriptional activator involved in organic acid metabolism, can improve plant growth and amino acid levels (Gln and Glu), reduce glucose levels, enhance nitrogen assimilation, and increase the nitrogen content in Arabidopsis[78]. Overexpression of ZmDof1 enhances nitrogen uptake, assimilation, and N and C levels in transgenic rice, leading to increased photosynthesis rates and biomass in the transgenic plants[79]. These findings demonstrate that Dof transcription factors are involved in regulating the nitrogen assimilation process in plants. This study found that 19 TF families may be involved in the regulation of the seven nitrogen assimilation-related genes in *L. ruthenicum*, with C2H2, Dof, GRAS, AP2, and BBR-BPC being the TF families with the most binding sites. Expression analysis and molecular docking suggest that *C2H2-63* likely plays a key role in maintaining nitrogen assimilation in *L.*

ruthenicum under salt stress, likely by promoting this process through its upregulated exxpression.

The adaptive evolutionary mechanism of LrFd-GOGAT

With the advancement of gene editing technologies, base editing techniques can rapidly and precisely improve specific genetic traits in crops[80]. Therefore, discovering loci associated with beneficial agronomic traits is of great importance in crop breeding. Black wolfberry, having long survived in desert saline-alkaline regions, exhibits strong adaptability to saline-alkaline environments[81]. This study found that the protein encoded by LrFd-GOGAT has seven amino acid sites under strong positive selection pressure. The p.Leu1322Phe mutation results in an additional helical structure between Phe1322 and Ser1327 in the LrFd-GOGAT protein, which may increase the stability of the FMN domain. In the Fd-GOGAT protein, there is an amino channel between the N-terminal amidotransferase domain and the FMN domain. The N-terminal amidotransferase domain marks the beginning of the amino channel and contains the binding site for L-glutamine. L-glutamine enters the amino channel via the N-terminal amidotransferase domain[82]. Under saline-alkaline conditions, protons are continuously pumped into the thylakoid lumen, but the alkaline conditions may inhibit the function of ATP synthase, preventing protons from effectively returning to the stroma through ATP synthase. This leads to a decrease in proton concentration in the chloroplast stroma and an increase in pH[83]. The isoelectric point of L-glutamine is 5.65, and as the pH of the chloroplast stroma increases, L-glutamine acquires more positive charges. The p.Glu223Ala and p.Ala391Phe mutations increase the electrostatic potential of the N-terminal amidotransferase domain, which may enhance the electrostatic attraction for L-glutamine under alkaline conditions[84], allowing L-glutamine to rapidly bind to the N-terminal amidotransferase, thereby improving the catalytic efficiency of LrFd-GOGAT. This is consistent with the results of molecular docking, which show that LrFd-GOGAT has a higher affinity for L-glutamine compared to LbFd-GOGAT.

Additionally, this study found that p.Ala883Thr and p.Leu1322Phe are located in unstructured loops, and their mutations increase the hydrophilicity of the corresponding regions. Meanwhile, p.Glu223Ala, p.Ala391Phe, p.Ser924Leu, p.Ser1353Ala, and p.Ser1573Cys are located in helical structures, and their mutations increase the hydrophobicity of the respective regions. Hydrophilic amino acids can typically form hydrogen bonds with water molecules and other polar molecules, thereby enhancing the solubility and stability of proteins under alkaline conditions[85]. In alkaline environments, the higher pH may affect the charge distribution and hydrogen bonding network of proteins, leading to the disruption of helical structures[86]. Mutations that increase hydrophobicity can enhance hydrophobic interactions within the helical core, thereby stabilizing the helical structure and preventing it from unwinding or unfolding under alkaline conditions[87]. Therefore, the mutations at these sites may also increase the hydrophilicity and stability of LrFd-GOGAT, which is beneficial for maintaining functional stability under alkaline conditions.

Conclusions

Through the identification and functional analysis of *GS*, *GOGAT*, and *GDH* genes in *Lycium* species, this study revealed the transcriptional regulatory patterns and evolutionary mechanisms of black wolfberry under salt stress. The genomes or transcriptomes of *Lycium* species contain two to four GS genes, two GOGAT genes, and three to four GDH genes. Under salt stress, the predominantly expressed GS genes in the black wolfberry family, *LrGS2* and *LrGS1.1*, were significantly upregulated after salt stress, and the expression of GOGAT genes was upregulated under severe salt stress. These results indicate that black wolfberry may accelerate the assimilation of NH_4^+ through the GS/GOGAT pathway to maintain nitrogen supply in both roots and leaves. In addition, the transcription factor C2H2-63 positively regulates the expression of nitrogen assimilation genes in black wolfberry, thereby participating in the regulation of nitrogen metabolism under salt stress. The study also identified mutations in the LrFd-GOGAT protein at specific amino acid sites, which may enhance the protein's stability and catalytic efficiency under alkaline conditions. These findings provide new insights for breeding crops with enhanced salt tolerance.

Author contributions

The authors confirm their contributions to the paper as follows: study conception and design: Qi J, Zhao J, Lu S, Ma Y, Du W, Zhang X; data collection: Qi J, Zhao J; analysis and interpretation of results: Qi J, Zhao J, Lu S, Ma Y, Zhou X, Song Q, Xing L; draft manuscript preparation: Qi J, Zhao J. All authors reviewed the results and approved the final version of the manuscript.

Data availability

All data generated or analyzed during this study are included in this published article and its supplementary information files.

Acknowledgments

This work was supported by grants from the Gansu Provincial Higher Education Support Program (Grant No. 2023CYZC-46), the Natural Science Foundation of Gansu Province (Grant No. 24JRRG016), the National Natural Science Foundation of China (Grant No. 32460055), the Scientific Research Startup Fund for Talent Introduction at Gansu Agricultural University (Grant No. GAU-KYQD-2021-36), and the Outstanding Doctoral Project of Gansu Provincial Science and Technology Program (25JRRA387).

Conflict of interest

The authors declare that they have no conflict of interest.

Supplementary information accompanies this paper at (https://www.maxapress.com/article/doi/10.48130/frures-0025-0025)

Dates

Received 7 January 2025; Revised 9 June 2025; Accepted 16 June 2025; Published online 26 August 2025

References

1. Haider S, Bibi K, Munyaneza V, Zhang H, Zhang W, et al. 2024. Drought-induced adaptive and ameliorative strategies in plants. *Chemosphere* 364:143134
2. Majidian P, Ghorbani H. 2024. Salinity stress in plants: challenges in view of physiological aspects. In *Abiotic Stress in Crop Plants - Ecophysiological Responses and Molecular Approaches*, eds Hasanuzzaman M, Nahar K. London: IntechOpen. doi: 10.5772/intechopen.114576
3. Li Z, Guan L, Zhang C, Zhang S, Liu Y, et al. 2024. Nitrogen assimilation genes in poplar: potential targets for improving tree nitrogen use efficiency. *Industrial Crops and Products* 216:118705
4. Li T, Chen X, Lin S. 2021. Physiological and transcriptomic responses to N-deficiency and ammonium: nitrate shift in *Fugacium kawagutii* (Symbiodiniaceae). *Science of The Total Environment* 753:141906

5. Kang J, Chu Y, Ma G, Zhang Y, Zhang X, et al. 2023. Physiological mechanisms underlying reduced photosynthesis in wheat leaves grown in the field under conditions of nitrogen and water deficiency. *The Crop Journal* 11:638−50
6. Ye JY, Tian WH, Jin CW. 2022. Nitrogen in plants: from nutrition to the modulation of abiotic stress adaptation. *Stress Biology* 2:4
7. Ullah A, Tariq A, Sardans J, Peñuelas J, Zeng F, et al. 2022. *Alhagi sparsifolia* acclimatizes to saline stress by regulating its osmotic, antioxidant, and nitrogen assimilation potential. *BMC Plant Biology* 22:453
8. Liu X, Hu B, Chu C. 2022. Nitrogen assimilation in plants: current status and future prospects. *Journal of Genetics and Genomics* 49:394−404
9. Huertas R, Ding N, Scheible W, Udvardi M. 2024. Transcriptional, metabolic, physiological and developmental responses to nitrogen limitation in switchgrass (*Panicum virgatum*). *Environmental and Experimental Botany* 222:105770
10. Zhang X, He P, Guo R, Huang K, Huang X. 2023. Effects of salt stress on root morphology, carbon and nitrogen metabolism, and yield of Tartary buckwheat. *Scientific Reports* 13:12483
11. Tian J, Pang Y, Yuan W, Peng J, Zhao Z. 2022. Growth and nitrogen metabolism in *Sophora Japonica* (L.) as affected by salinity under different nitrogen forms. *Plant Science* 322:111347
12. Huang J, Zhu C, Hussain S, Huang J, Liang Q, et al. 2020. Effects of nitric oxide on nitrogen metabolism and the salt resistance of rice (*Oryza Sativa* L.) seedlings with different salt tolerances. *Plant Physiology and Biochemistry* 155:374−83
13. Zhang Y, Zhang L, Hu XH. 2014. Exogenous spermidine-induced changes at physiological and biochemical parameters levels in tomato seedling grown in saline-alkaline condition. *Botanical Studies* 55:58
14. Krapp A. 2015. Plant nitrogen assimilation and its regulation: a complex puzzle with missing pieces. *Current Opinion in Plant Biology* 25:115−22
15. Shao QS, Shu S, Du J, Xing WW, Guo SR, et al. 2015. Effects of NaCl stress on nitrogen metabolism of cucumber seedlings. *Russian Journal of Plant Physiology* 62:595−603
16. Meng S, Su L, Li Y, Wang Y, Zhang C, et al. 2016. Nitrate and ammonium contribute to the distinct nitrogen metabolism of *Populus simonii* during moderate salt stress. *PLoS One* 11:e0150354
17. Ullah A, Li M, Noor J, Tariq A, Liu Y, et al. 2019. Effects of salinity on photosynthetic traits, ion homeostasis and nitrogen metabolism in wild and cultivated soybean. *PeerJ* 7:e8191
18. Ben Azaiez FE, Ayadi S, Capasso G, Landi S, Paradisone V, et al. 2020. Salt stress induces differentiated nitrogen uptake and antioxidant responses in two contrasting barley landraces from *MENA* region. *Agronomy* 10:1426
19. Wang M, Gong S, Fu L, Hu G, Li G, et al. 2022. The involvement of antioxidant enzyme system, nitrogen metabolism and osmoregulatory substances in alleviating salt stress in inbred maize lines and hormone regulation mechanisms. *Plants* 11:1547
20. Mondal R, Kumar A, Chattopadhyay SK. 2021. Structural property, molecular regulation, and functional diversity of glutamine synthetase in higher plants: a data-mining bioinformatics approach. *The Plant Journal* 108:1565−84
21. Fernandes I, Paulo OS, Marques I, Sarjkar I, Sen A, et al. 2022. Salt stress tolerance in *Casuarina* Glauca: insights from the branchlets transcriptome. *Plants* 11:2942
22. López-Arredondo DL, Leyva-González MA, Alatorre-Cobos F, Herrera-Estrella L. 2013. Biotechnology of nutrient uptake and assimilation in plants. *The International Journal Of Developmental Biology* 57:595−610
23. Li F, Li H, Li S, He Z. 2024. A review of *Lycium ruthenicum* Murray: geographic distribution tracing, bioactive components, and functional properties. *Heliyon* 10:e39566
24. Qin X, Yin Y, Zhao J, An W, Fan Y, et al. 2022. Metabolomic and transcriptomic analysis of *Lycium* Chinese and *L. ruthenicum under salinity stress*. *BMC Plant Biology* 22:8
25. Li W, Rao S, Du C, Liu L, Dai G, et al. 2022. Strategies used by two goji species, *Lycium ruthenicum* and *Lycium barbarum*, to defend against salt stress. *Scientia Horticulturae* 306:111430
26. Chen Y, Huang W, Zhang F, Luo X, Hu B, et al. 2021. Metabolomic profiling of Dongxiang wild rice under salinity demonstrates the significant role of amino acids in rice salt stress. *Frontiers in Plant Science* 12:729004
27. Grabherr MG, Haas BJ, Yassour M, Levin JZ, Thompson DA, et al. 2011. Full-length transcriptome assembly from RNA-seq data without a reference genome. *Nature Biotechnology* 29:644−52
28. Minh BQ, Schmidt HA, Chernomor O, Schrempf D, Woodhams MD, et al. 2020. IQ-TREE 2: new models and efficient methods for phylogenetic inference in the genomic era. *Molecular Biology and Evolution* 37:1530−34
29. Hu B, Jin J, Guo AY, Zhang H, Luo J, et al. 2015. GSDS 2.0: an upgraded gene feature visualization server. *Bioinformatics* 31:1296−97
30. Jin J, Tian F, Yang DC, Meng YQ, Kong L, et al. 2017. PlantTFDB 4.0: toward a central hub for transcription factors and regulatory interactions in plants. *Nucleic Acids Research* 45:D1040−D1045
31. Cline MS, Smoot M, Cerami E, Kuchinsky A, Landys N, et al. 2007. Integration of biological networks and gene expression data using Cytoscape. *Nature Protocols* 2:2366−82
32. Abramson J, Adler J, Dunger J, Evans R, Green T, et al. 2024. Accurate structure prediction of biomolecular interactions with AlphaFold 3. *Nature* 630:493−500
33. PyMOL. *The PyMOL Molecular Graphics System*, Version 3.0. Schrödinger, LLC
34. Wei J, Tiika RJ, Ma Y, Yang H, Cui G, et al. 2022. Transcriptome-wide identification and analysis of the KT/HAK/KUP family in black goji under NaCl stress. *Agronomy Journal* 114:2069−80
35. Kim D, Paggi JM, Park C, Park C, Bennett C, Salzberg SL. 2019. Graph-based genome alignment and genotyping with HISAT2 and HISAT-genotype. *Nature Biotechnology* 37:907−15
36. Liao Y, Smyth GK, Shi W. 2014. FeatureCounts: an efficient general purpose program for assigning sequence reads to genomic features. *Bioinformatics* 30:923−30
37. Love MI, Huber W, Anders S. 2014. Moderated estimation of fold change and dispersion for RNA-seq data with DESeq2. *Genome Biology* 15:550
38. Yang C, Shen S, Zhou S, Li Y, Mao Y, et al. 2022. Rice metabolic regulatory network spanning the entire life cycle. *Molecular Plant* 15:258−75
39. Qi J, Luo Y, Huang H, Lu S, Zhao F, et al. 2023. Molecular mechanism of response and adaptation of antioxidant enzyme system to salt stress in leaves of *Gymnocarpos przewalskii*. *Plants* 12:3370
40. Yang Z. 2007. PAML 4: phylogenetic analysis by maximum likelihood. *Molecular Biology and Evolution* 24:1586−91
41. Webb B, Sali A. 2016. Comparative protein structure modeling using MODELLER. *Current Protocols in Bioinformatics* 54:5.6.1−5.6.37
42. Pettersen EF, Goddard TD, Huang CC, Couch GS, Greenblatt DM, et al. 2004. UCSF *Chimera* - a visualization system for exploratory research and analysis. *Journal of Computational Chemistry* 25:1605−12
43. Ittisoponpisan S, Islam SA, Khanna T, Alhuzimi E, David A, et al. 2019. Can predicted protein 3D structures provide reliable insights into whether missense variants are disease associated? *Journal of Molecular Biology* 431:2197−212
44. Forli S, Huey R, Pique ME, Sanner MF, Goodsell DS, et al. 2016. Computational protein–ligand docking and virtual drug screening with the AutoDock suite. *Nature Protocols* 11:905−19
45. Zhang W, Yuan S, Liu N, Zhang H, Zhang Y. 2024. Glutamine synthetase and glutamate synthase family perform diverse physiological functions in exogenous hormones and abiotic stress responses in *Pyrus betulifolia* Bunge (*P.be*). *Plants* 13:2759
46. Zeng DD, Qin R, Li M, Alamin M, Jin XL, et al. 2017. The ferredoxin-dependent glutamate synthase (OsFd-GOGAT) participates in leaf senescence and the nitrogen remobilization in rice. *Molecular Genetics And Genomics* 292:385−95
47. Gonnet S, Díaz P. 2000. Glutamine synthetase and glutamate synthase activities in relation to nitrogen fixation in *Lotus* spp. *Revista Brasileira de Fisiologia Vegetal* 12:195−202
48. Liu Z, Zhu YA, Dong Y, Tang L, Zheng Y, et al. 2021. Interspecies interaction for nitrogen use efficiency *via* up-regulated glutamine and glutamate synthase under wheat-faba bean intercropping. *Field Crops Research* 274:108324
49. Liu L, Wang J, Han Z, Sun X, Li H, et al. 2016. Molecular analyses of tomato *GS*, GOGAT and GDH gene families and their response to abiotic stresses. *Acta Physiologiae Plantarum* 38:229

50. García-Gutiérrez Á, Cánovas FM, Ávila C. 2018. Glutamate synthases from conifers: gene structure and phylogenetic studies. *BMC Genomics* 19:65
51. Tabuchi M, Abiko T, Yamaya T. 2007. Assimilation of ammonium ions and reutilization of nitrogen in rice (*Oryza sativa* L.). *Journal of Experimental Botany* 58:2319–27
52. Cao L, Xu C, Sun Y, Niu C, Leng X, et al. 2023. Genome-wide identification of glutamate synthase gene family and expression patterns analysis in response to carbon and nitrogen treatment in *Populus*. *Gene* 851:146996
53. Qiao Z, Chen M, Ma W, Zhao J, Zhu J, et al. 2024. Genome-wide identification and expression analysis of *GS* and *GOGAT* gene family in Pecan (*Carya illinoinensis*) under different nitrogen forms. *Phyton* 93:2349–65
54. Li S, Jiao B, Wang J, Zhao P, Dong F, et al. 2024. Identification of wheat glutamate synthetase gene family and expression analysis under nitrogen stress. *Genes* 15:827
55. Swarbreck SM, Defoin-Platel M, Hindle M, Saqi M, Habash DZ. 2011. New perspectives on glutamine synthetase in grasses. *Journal of Experimental Botany* 62:1511–22
56. Ding S, Lv J, Hu Z, Wang J, Wang P, et al. 2023. Phytosulfokine peptide optimizes plant growth and defense via glutamine synthetase GS2 phosphorylation in tomato. *The EMBO Journal* 42:e111858
57. Yu Y, Kou X, Gao R, Chen X, Zhao Z, et al. 2021. Glutamine Synthetases Play a Vital Role in High Accumulation of Theanine in Tender Shoots of Albino Tea Germplasm "Huabai 1". *Journal of Agricultural and Food Chemistry* 69:13904–13915
58. Freedman AH, Clamp M, Sackton TB. 2021. Error, noise and bias in *de novo* transcriptome assemblies. *Molecular Ecology Resources* 21:18–29
59. Tang D, Jiao Z, Zhang Q, Liu MY, Ruan J. 2021. Glutamate dehydrogenase isogenes *CsGDHs* cooperate with glutamine synthetase isogenes *CsGSs* to assimilate ammonium in tea plant (*Camellia sinensis* L.). *Plant Science* 312:111031
60. Grzechowiak M, Sliwiak J, Link A, Ruszkowski M. 2024. Legume-type glutamate dehydrogenase: structure, activity, and inhibition studies. *International Journal of Biological Macromolecules* 278:134648
61. Tercé-Laforgue T, Clément G, Marchi L, Restivo FM, Lea PJ, et al. 2015. Resolving the role of plant NAD-glutamate dehydrogenase: III. Overexpressing individually or simultaneously the two enzyme subunits under salt stress induces changes in the leaf metabolic profile and increases plant biomass production. *Plant and Cell Physiology* 56:1918–29
62. Fontaine JX, Tercé-Laforgue T, Armengaud P, Clément G, Renou JP, et al. 2012. Characterization of a NADH-Dependent Glutamate Dehydrogenase Mutant of *Arabidopsis* demonstrates the key role of this enzyme in root carbon and nitrogen metabolism. *The Plant Cell* 24:4044–65
63. Inokuchi R, Kuma KI, Miyata T, Okada M. 2002. Nitrogen-assimilating enzymes in land plants and algae: phylogenic and physiological perspectives. *Physiologia Plantarum* 116:1–11
64. Xu Y, Zhang K, Li S, Zhou Y, Ran S, et al. 2023. Carbon and nitrogen metabolism in tomato (*Solanum lycopersicum* L.) leaves response to nitrogen treatment. *Plant Growth Regulation* 100:747–56
65. Rana V, Ram S, Nehra K, Sharma I. 2016. Expression of genes related to Na^+ exclusion and proline accumulation in tolerant and susceptible wheat genotypes under salt stress. *Cereal Research Communications* 44:404–13
66. Xu G, Fan X, Miller AJ. 2012. Plant nitrogen assimilation and use efficiency. *Annual Review of Plant Biology* 63:153–82
67. Fortunato S, Nigro D, Lasorella C, Marcotuli I, Gadaleta A, et al. 2023. The role of glutamine synthetase (GS) and glutamate synthase (GOGAT) in the improvement of nitrogen use efficiency in cereals. *Biomolecules* 13:1771
68. Kiba T, Krapp A. 2016. Plant nitrogen acquisition under low availability: regulation of uptake and root architecture. *Plant and Cell Physiology* 57:707–14
69. Ma J, Cirillo V, Zhang D, Maggio A, Wang L, et al. 2020. Regulation of ammonium cellular levels is an important adaptive trait for the euhalophytic behavior of *Salicornia europaea*. *Plants* 9:257
70. Dubey RS, Srivastava RK, Pessarakli M. 2021. Physiological mechanisms of nitrogen absorption and assimilation in plants under stressful conditions. In *Handbook of Plant and Crop Physiology*, 4th edition. Boca Raton, FL: CRC Press. pp. 579–616 doi: 10.1201/9781003093640-36
71. Hoshida H, Tanaka Y, Hibino T, Hayashi Y, Tanaka A, et al. 2000. Enhanced tolerance to salt stress in transgenic rice that overexpresses chloroplast glutamine synthetase. *Plant Molecular Biology* 43:103–11
72. Hao R, Gao Z, Zhang X, Wang X, Ye W, et al. 2025. A large-scale gene co-expression network analysis reveals Glutamate Dehydrogenase 2 (GhGDH2_D03) as a hub regulator of salt and salt-alkali tolerance in cotton. *Plant Molecular Biology* 115:54
73. Wang Y, Li E, Yu N, Wang X, Cai C, et al. 2012. Characterization and expression of glutamate dehydrogenase in response to acute salinity stress in the Chinese mitten crab, *Eriocheir sinensis*. *PLoS One* 7:e37316
74. Ochieng WA, Muthui SW, Xian L, Linda EL, Kombe CA, et al. 2024. Mechanisms of ammonium detoxification in submerged macrophytes under shade conditions. *Science of The Total Environment* 951:175795
75. Huang Z, Zhao L, Chen D, Liang M, Liu Z, et al. 2013. Salt stress encourages proline accumulation by regulating proline biosynthesis and degradation in Jerusalem artichoke plantlets. *PLoS One* 8:e62085
76. Gaudinier A, Rodriguez-Medina J, Zhang L, Olson A, Liseron-Monfils C, et al. 2018. Transcriptional regulation of nitrogen-associated metabolism and growth. *Nature* 563:259–64
77. Chen Y, Yang M, Ding W, Zhao Y, Li X, et al. 2017. Wheat ZFP gene TaZFP593;I mediates the N-starvation adaptation of plants through regulating N acquisition and the ROS metabolism. *Plant Cell, Tissue and Organ Culture* 129:271–88
78. Yanagisawa S, Akiyama A, Kisaka H, Uchimiya H, Miwa T. 2004. Metabolic engineering with Dof1 transcription factor in plants: improved nitrogen assimilation and growth under low-nitrogen conditions. *Proceedings of the National Academy of Sciences of the United States of America* 101:7833–38
79. Kurai T, Wakayama M, Abiko T, Yanagisawa S, Aoki N, et al. 2011. Introduction of the ZmDof1 gene into rice enhances carbon and nitrogen assimilation under low - nitrogen conditions. *Plant Biotechnology Journal* 9:826–37
80. Zhang Y, Pribil M, Palmgren M, Gao C. 2020. A CRISPR way for accelerating improvement of food crops. *Nature Food* 1:200–205
81. Yisilam G, Wang CX, Xia MQ, Comes HP, Li P, et al. 2022. Phylogeography and population genetics analyses reveal evolutionary history of the desert resource plant *Lycium ruthenicum* (Solanaceae). *Frontiers in Plant Science* 13:915526
82. van den Heuvel RHH, Svergun DI, Petoukhov MV, Coda A, Curti B, et al. 2003. The active conformation of glutamate synthase and its binding to ferredoxin. *Journal of Molecular Biology* 330:113–28
83. Foyer CH, Shigeoka S. 2011. Understanding oxidative stress and antioxidant functions to enhance photosynthesis. *Plant Physiology* 155:93–100
84. Garcia-Viloca M, Gao J, Karplus M, Truhlar DG. 2004. How enzymes work: analysis by modern rate theory and computer simulations. *Science* 303:186–95
85. Gao K, Rao J, Chen B. 2024. Plant protein solubility: a challenge or insurmountable obstacle. *Advances in Colloid and Interface Science* 324:103074
86. Yang Y, Zhao Y, Xu M, Yao Y, Wu N, et al. 2020. Effects of strong alkali treatment on the physicochemical properties, microstructure, protein structures, and intermolecular forces in egg yolks, plasma, and granules. *Food Chemistry* 311:125998
87. Pace CN, Treviño S, Prabhakaran E, Scholtz JM. 2004. Protein structure, stability and solubility in water and other solvents. *Philosophical Transactions of the Royal Society B* 359:1225–35